Intermolecular C−H Activation of Hydrocarbons by Tungsten Alkylidene Complexes: An Experimental and Computational Mechanistic Study

Craig S. Adams, Peter Legzdins,* and W. Stephen McNeil

Department of Chemistry, The University of British Columbia, Vancouver, British Columbia, Canada V6T 1Z1

Received May 9, 2001

$Cp^*W(NO)(CH_2CMe_3)_2$ (**1**) and $Cp^*W(NO)(CH_2CMe_3)(CH_2C_6H_5)$ (**2**) under moderate conditions (70 °C, 40 h) generate the reactive complexes $Cp^*W(NO)(=CHCMe_3)$ (**A**) and $Cp^*W(NO)(=CHC_6H_5)$ (**B**), respectively, which activate hydrocarbon solvents via the addition of C−H across the M=C bond. The α-deuterated derivative $Cp^*W(NO)(CD_2CMe_3)_2$ (**1-*d*$_4$**) undergoes intramolecular H/D exchange within the neopentyl ligands, consistent with the formation of σ-neopentane complexes prior to neopentane elimination. The thermolysis of **1** in a 1:1 molar mixture of tetramethylsilane-h_{12} and tetramethylsilane-d_{12} (70 °C, 40 h) yields an intermolecular KIE of 1.07(4):1. Thermolysis of **1** and **2** in 1:1 benzene/benzene-d_6 yields intermolecular KIEs of 1.03(5):1 and 1.17(19):1, respectively. The KIE values are inconsistent with rate-determining C−H bond addition to the M=C linkage and indicate that coordination of the substrate to the metal center is the discriminating factor in alkane and arene intermolecular competitions. The complexes $Cp^*W(NO)(CH_2CMe_3)(C_6D_5)$ (**5-*d*$_5$**) and $Cp^*W(NO)(CH_2C_6H_5)(C_6D_5)$ (**6-*d*$_5$**) convert to the respective H/D scrambled products $Cp^*W(NO)(CHD_{syn}CMe_3)(C_6D_4H_1)$ (**5′-*d*$_5$**) and $Cp^*W(NO)(CHD_{syn}C_6H_5)(C_6D_4H_1)$ (**6′-*d*$_5$**) under thermolytic conditions, consistent with the occurrence of reversible aromatic sp^2 C−H bond cleavage. The results suggest that the previously reported discrimination between the aryl and benzyl products of toluene activation by **A** and **B** originates from coordination of toluene to the metal center in two distinct modes. Supporting DFT calculations on the activation of toluene by $CpW(NO)(=CH_2)$ (**C**) indicate that aromatic sp^2 C−H bond activation proceeds through a π-arene complex, while benzylic sp^3 C−H bond activation proceeds through a $\eta^2(C,H)$,σ-phenylmethane complex. The principal factor behind the preferential formation of the aryl products appears to be the relative energies of formation of these intermediates.

Introduction

The development of soluble organometallic complexes as reagents for the selective activation of C−H bonds remains an area of intense research activity.[1] Over the past 30 years, a diverse array of lanthanide, actinide, and transition-metal complexes has been found to activate hydrocarbon substrates such as alkanes and arenes. Several representative complexes have been studied in great detail by both experimental and theoretical methods, and accordingly, in each case the principal factors that govern the activation of a C−H bond have been identified.[2−4] In large part due to these investigations, the utility of this class of reagents has begun to be realized in synthetic organic applications.[5]

For the past few years, we have been studying a new and rare type of intermolecular C−H activation chemistry that is derived from the thermal behavior of $Cp^*W(NO)(CH_2CMe_3)_2$ (**1**) and $Cp^*W(NO)(CH_2CMe_3)(CH_2C_6H_5)$ (**2**).[6,7] Under moderate conditions (70 °C, 40 h), **1** and **2** generate the respective alkylidene complexes $Cp^*W(NO)(=CHCMe_3)$ (**A**) and $Cp^*W(NO)(=CHC_6H_5)$ (**B**), which activate the C−H bonds of hydrocarbon solvents via addition across the metal−carbon double

(1) (a) Shilov, A. E.; Shul'pin, G. B. *Activation and Catalytic Reactions of Saturated Hydrocarbons in the Presence of Metal Complexes*; Kluwer Academic: Dordrecht, The Netherlands, 2000. (b) Arndtsen, B. A.; Bergman, R. G.; Mobley, T. A.; Peterson, T. H. *Acc. Chem. Res.* **1995**, *28*, 154−162. (c) Crabtree, R. H. *Chem. Rev.* **1995**, *95*, 987−1007. (d) Stahl, S. S.; Labinger, J. A.; Bercaw, J. E. *Angew. Chem., Int. Ed. Engl.* **1998**, *37*, 2180−2192.

(2) For example, see: (a) Peterson, T. H.; Golden, J. T.; Bergman, R. G. *J. Am. Chem. Soc.* **2001**, *123*, 455−462 and refs 1−27 and 32−35 therein.

(3) Stahl, S. S.; Labinger, J. A.; Bercaw, J. E. *J. Am. Chem. Soc.* **1996**, *118*, 5961−5976 and refs 8−21 therein.

(4) Slaughter, L. M.; Wolczanski, P. T.; Klinckman, T. R.; Cundari, T. R. *J. Am. Chem. Soc.* **2000**, *122*, 7953−7975 and refs 10−17 therein.

(5) For an inspiring illustration of this fact, see: Johnson, J. A.; Sames, D. *J. Am. Chem. Soc.* **2000**, *122*, 6321−6322.

(6) (a) Tran, E.; Legzdins, P. *J. Am. Chem. Soc.* **1997**, *119*, 5071−5072. (b) Adams, C. S.; Legzdins, P.; Tran, E. *J. Am. Chem. Soc.* **2001**, *123*, 612−624.

(7) For the three other reported examples of intermolecular C−H activations by alkylidene complexes, see: (a) Coles, M. P.; Gibson, V. C.; Clegg, W.; Elsegood, M. R. J.; Porrelli, P. A. *J. Chem. Soc., Chem. Commun.* **1996**, 1963−1964. (b) van der Heijden, H.; Hessen, B. *J. Chem. Soc., Chem. Commun.* **1995**, 145−146. (c) Cheon, J.; Rogers, D. M.; Girolami, G. S. *J. Am. Chem. Soc.* **1997**, *119*, 6804−6813.

10.1021/om010380c CCC: $20.00
Publication on Web 10/12/2001

Scheme 1

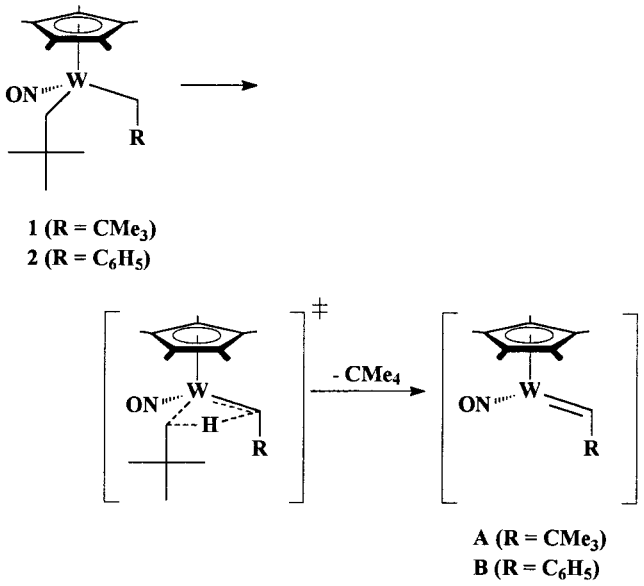

bond. These are the only alkylidene complexes known to activate both alkane and arene substrates and as such are prototypical complexes for investigations into this novel mode of intermolecular C−H bond activation.

Our understanding of the activation chemistry derived from **1** and **2** is, however, incomplete. For example, the exact mechanism by which the alkylidene complexes are formed has not yet been resolved. Our initial kinetic and labeling studies conclusively established that formation of **A** and **B** involves the intramolecular rate-determining cleavage of an α-C−H bond and the formation of neopentane. Consequently, we proposed the simple α-H abstraction mechanism shown in Scheme 1.[6b]

Recently, however, it has been suggested that the actual mechanism may be more complicated.[8] Poli and Smith have conducted DFT calculations on the transformation of the model compound $CpW(NO)(CH_3)_2$ (**3**) to the methylidene complex $CpW(NO)(=CH_2)$ (**C**). The results indicate that the formation of **C** does indeed begin with a metal-assisted, intramolecular α-H abstraction with a late transition state in which M=C bond formation is essentially complete. To this point, the calculations agree with our proposed mechanism, and a third plausible mechanism involving rate-determining α-H elimination to a discrete metal hydride intermediate can be ruled out.[9] Intriguingly, though, Poli and Smith located a discrete hydrocarbon complex intermediate after the α-H abstraction, namely a methane η^2(C,H),σ complex[10] (Scheme 2). Hence, the mechanism suggested by these calculations consists of rate-limiting α-H abstraction from **1** or **2**, followed by neopentane elimination from a transient σ-neopentane intermediate to form the reactive alkylidene species **A** and **B**.

By microscopic reversibility arguments, the mechanism of formation of **A** and **B** is intimately linked to the mechanism by which **A** and **B** activate substrate

Scheme 2

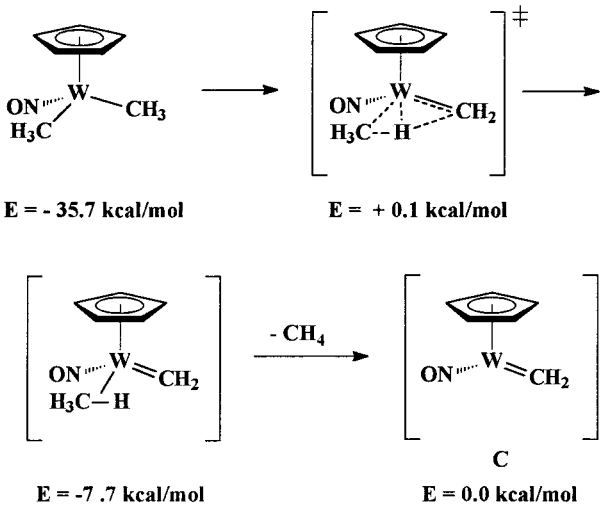

C−H bonds. Thus, resolving whether hydrocarbon complexes exist as intermediates prior to and after the formation of **A** and **B** and the role these intermediates play, if any, in the activation process is critical to advancing our understanding of the observed chemistry. Herein, we report on our experimental mechanistic studies directed specifically toward probing the proposed intermediacy of hydrocarbon complexes. We also report subsequent experimental and theoretical work that reveals additional mechanistic details regarding the activation of aliphatic and arene C−H bonds by **A** and **B**. Taken together, these studies provide a general picture of the C−H activation chemistry mediated by these alkylidene complexes.

Results and Discussion

I. Hydrocarbon Complexes in the Formation of the Alkylidene Complex. Intermediate hydrocarbon complexes are commonly detected indirectly via the observation of intramolecular H/D scrambling in the ligands involved in hydrocarbon elimination reactions.[11,12] Thermolysis of the α-deuterated analogue of **1**, namely $Cp^*W(NO)(CD_2CMe_3)_2$ (**1-*d*$_4$**), in select aliphatic and aromatic solvents likewise indicates that σ-neopentane complexes are being formed prior to neopentane elimination.

For example, NMR analysis of the thermolysis of **1-*d*$_4$** in tetramethylsilane at 70 °C for 90 h reveals the

(8) Poli, R.; Smith, K. M. *Organometallics* **2000**, *19*, 2858−2867.
(9) McDade, C.; Green, J. C.; Bercaw, J. E. *Organometallics* **1982**, *1*, 1629−1634.
(10) Hall, C.; Perutz, R. N. *Chem. Rev.* **1996**, *96*, 3125−3146.

(11) (a) Feher, F. J.; Jones, W. D. *J. Am. Chem. Soc.* **1984**, *106*, 1650−1663. (b) Jones, W. D.; Feher, F. J. *J. Am. Chem. Soc.* **1986**, *108*, 4814−4819. (c) Selmeczy, A. D.; Jones, W. D.; Osman, R.; Perutz, R. N. *Organometallics* **1995**, *14*, 5677−5685. (d) Jones, W. D.; Hessel, E. T. *J. Am. Chem. Soc.* **1992**, *114*, 6087−6095. (e) Wick, D. D.; Reynolds, K. A.; Jones, W. D. *J. Am. Chem. Soc.* **1999**, *121*, 3974−3983. (f) Schaefer, D. F., II; Wolczanski, P. T. *J. Am. Chem. Soc.* **1998**, *120*, 4881−4882. (g) Periana, R. A.; Bergman, R. G. *J. Am. Chem. Soc.* **1986**, *108*, 7346−7355. (h) Stoutland, P. O.; Bergman, R. G. *J. Am. Chem. Soc.* **1988**, *110*, 5732−5744. (i) McGhee, W. D.; Bergman, R. G. *J. Am. Chem. Soc.* **1988**, *110*, 4246−4262. (j) Mobley, T. A.; Schade, C.; Bergman, R. G. *Organometallics* **1998**, *17*, 3574−3587.

(12) (a) Bullock, R. M.; Headford, C. E. L.; Hennessy, K. M.; Kegley, S. E.; Norton, J. E. *J. Am. Chem. Soc.* **1989**, *111*, 3897−3908. (b) Parkin, G.; Bercaw, J. E. *Organometallics* **1989**, *8*, 1172−1179. (c) Gould, G. L.; Heinekey, D. M. *J. Am. Chem. Soc.* **1989**, *111*, 5502−5504. (e) Gross, C. L.; Girolami, G. S. *J. Am. Chem. Soc.* **1998**, *120*, 6605−6606. (f) Chernega, A.; Cook, J.; Green, M. L. H.; Labella, L.; Simpson, S. J.; Souter, J.; Stephens, A. H. H. *J. Chem. Soc., Dalton Trans.* **1997**, 3225−3243.

production of both Cp*W(NO)($CH_{syn}DCMe_3$)(CH_2SiMe_3) (**4-d_1**) and Cp*W(NO)(CH_2CMe_3-d_x)(CH_2SiMe_3) (**4′-d_x**, $0 \le x \le 4$ (vide infra))[13] (eq 1). Diagnostic features of

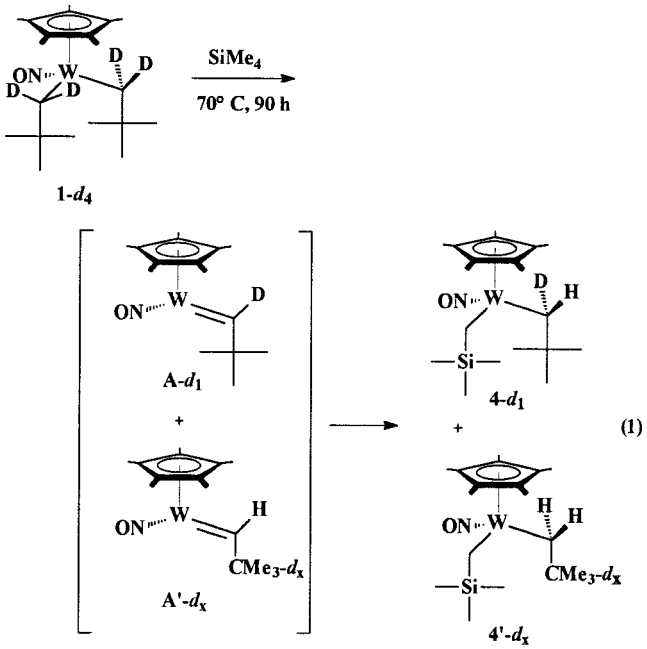

4-d_1 in the ^{1}H (C_6D_6) NMR and ^{2}H{^{1}H} (C_6H_6) spectra are the doublets attributable to the syn and anticlinal[14] methylene protons of the (trimethylsilyl)methyl ligand and the singlets arising from the syn and anticlinal methylene proton and deuteron of the neopentyl ligand. Diagnostic features of **4′-d_x** in the ^{1}H (C_6D_6) NMR spectrum are the two diastereotopic methylene doublets for the neopentyl ligand and a decrease in intensity of the combined *tert*-butyl resonances relative to the Cp* signal. The latter feature is matched by the presence of a strong singlet in the ^{t}Bu region in the ^{2}H{^{1}H} (C_6H_6) NMR spectrum.

The complex **4-d_1** is the expected product of C−H activation by the α-D neopentylidene complex derived by direct elimination of neopentane **1-d_4**, namely Cp*W(NO)(=CDCMe$_3$) (**A-d_1**). On the other hand, complex **4′-d_x** is clearly derived from the C−H activation of tetramethylsilane by an α-H alkylidene complex with deuterium in the ^{t}Bu group, namely Cp*W(NO)(=CH-CMe_3-d_x) (**A′-d_x**). The intermediate **A′-d_x**, in turn, is the expected result of H/D scrambling in the neopentyl ligands of **1-d_4** prior to neopentane elimination. Integration of appropriate signals in the ^{1}H (C_6D_6) NMR spectrum indicates that ∼48% of the total product is **4′-d_x**, thereby confirming that approximately half of **1-d_4** undergoes H/D exchange to form **A′-d_x** during the thermolysis. Moreover, on average, slightly less than three deuterium atoms are exchanged into the ^{t}Bu group of **A′-d_x** and **4′-d_x** ($x \cong 2.8$ in CMe_3-d_x) (see Experimental Section for details).

(13) Throughout this manuscript, a prime after a compound number (i.e. **4-d_1**) is used to denote an isotopomer of the parent compound that is formed via intramolecular H/D exchange (i.e. **4′-d_1**).

(14) The synclinal and anticlinal orientations of the methylene protons are defined with respect to the other M−C bond in the preferred stereochemistry in which both alkyl ligands are pointing away from the Cp* ligand.

Table 1. Average Relative Intensities of Mass Spectral Peaks Derived from Neopentane

	rel *m/z* peak intensity				
sample	57	58	59	60	61
neopentane-d_3[a]	33	1.47	0	100	4.4
from **1-d_4** in tetramethylsilane	48.3	54.6	9.7	100	5.6
from **1-d_4** in benzene-d_6	47.5	56.4	12.3	100	6.8

[a] Reference 7c.

Table 2. Calculated Distributions of Neopentane Isotopomers Generated in the Thermolyses of 1-d_4

	neopentane isotomer distribn (%)				
solvent	d_0	d	d_2	d_3	d_4
tetramethylsilane	(−0.5)	31.6	4.9	63.3	0.6
benzene-d_6	(−1.5)	31.8	6.4	61.8	1.6

The thermolysis of **1-d_4** in benzene-d_6 likewise generates products consistent with C−D activation by both **A-d_1** and **A′-d_x** (eq 2). The ^{2}H{^{1}H} (C_6H_6) NMR spectrum of the product mixture has unique signals attributable to Ph−D and D_{anti} of Cp*W(NO)(CD_2CMe_3)-

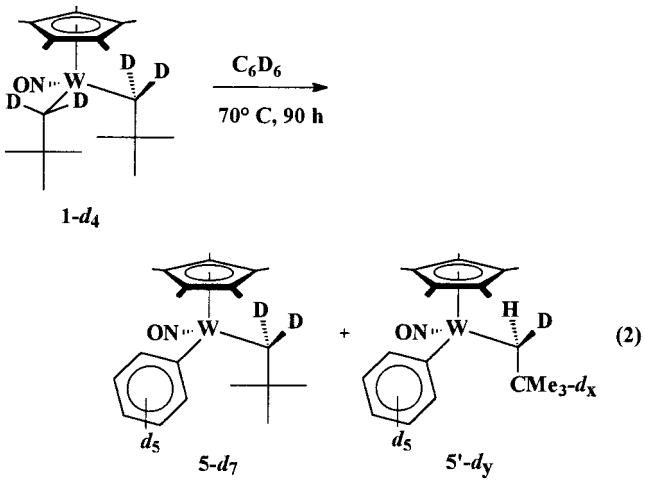

(Ph-d_5) (**5-d_7**) derived from **A-d_1**. Additionally, there are overlapping resonances for D_{syn} of **5-d_7** and Cp*W(NO)-($CHD_{syn}CMe_3$-d_x)(Ph-d_5) (**5′-d_y**), as well as a ^{t}Bu−D resonance for **5′-d_y**. To match, there is a singlet resonance for H_{anti} of **5′-d_y** in the ^{1}H (C_6D_6) NMR spectrum. Integration of appropriate signals in the ^{1}H (C_6D_6) NMR spectrum reveals that similar amounts of H/D exchange are occurring in benzene-d_6 and tetramethylsilane (i.e. $y = x + 6$).

GC/MS analysis of the volatile organics from the two thermolyses provides additional evidence for H/D exchange in the neopentyl ligands of **1-d_4** prior to neopentane elimination. The observed MS fragmentation patterns of the *tert*-butyl ions from neopentane clearly indicate that other neopentane isotopomers are being formed in addition to neopentane-d_3 (Table 1). A 5 × 5 matrix analysis of the peak intensities[7c] estimates the composition to be primarily neopentane-d_3 and neopentane-d_1, with small amounts of neopentane-d_2 and neopentane-d_4 (Table 2; see Experimental Section for details).[15]

Finally, H/D exchange can be observed directly by spectroscopic monitoring. To illustrate, the results obtained from monitoring the thermolysis of **1-d_4** in

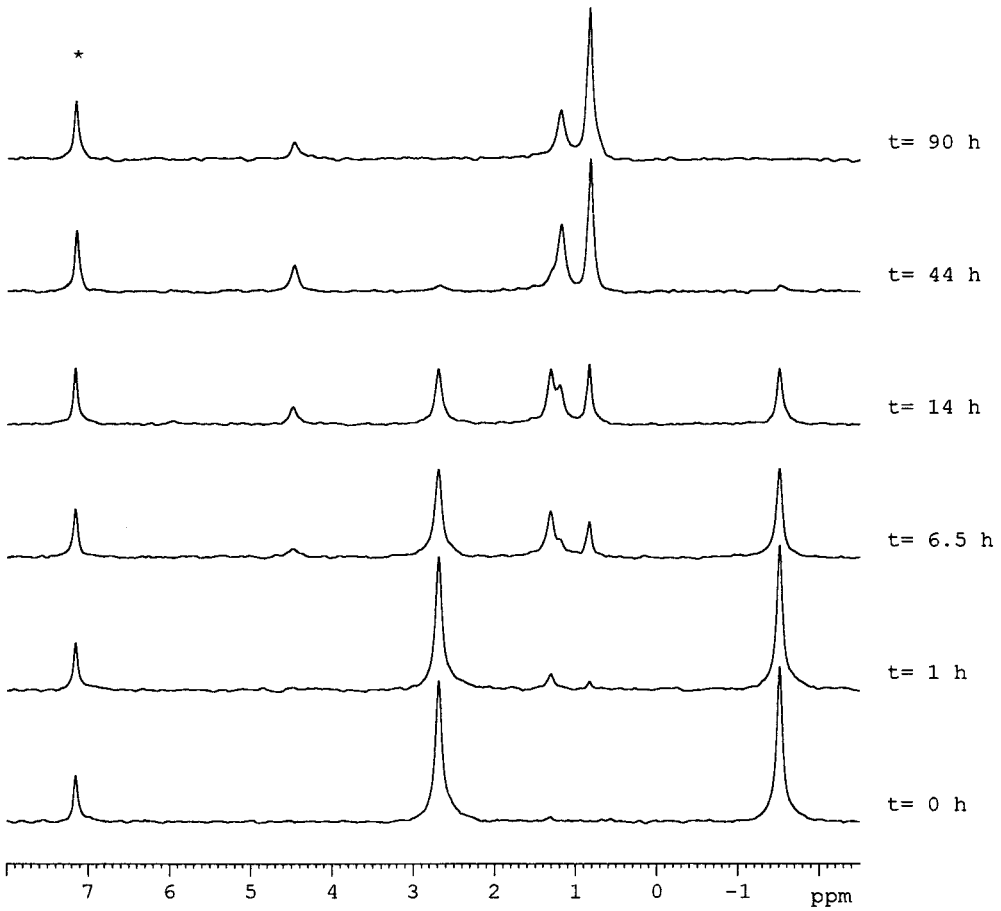

Figure 1. $^2H\{^1H\}$ (C_6H_6) NMR spectra from the thermolysis of **1-*d*$_4$** in benzene-d_6 over 90 h at 70 °C (the asterisk denotes the solvent peak).

benzene by $^2H\{^1H\}$ (C_6H_6) NMR spectroscopy are shown in Figure 1. Initially, a small resonance for deuterium in the *tert*-butyl moiety of **1-*d*$_4$** is observable at 1.30 ppm, along with the expected strong resonances from the deuterium label in the synclinal and anticlinal methylene positions at −1.51 and 2.69 ppm, respectively. After 1 h, the intensity of the signal at 1.30 ppm increases noticeably, while a new signal attributable to free deuterated neopentane is observed at 0.83 ppm, consistent with concomitant H/D exchange and product formation. After 14 h, new signals are clearly visible for the D_{anti} (4.49 ppm) and ^{t}Bu−D moieties (1.18 ppm) of the respective products Cp*W(NO)($CH_{syn}DCMe_3$)(Ph-h_5) (**5-*d*$_1$**) and Cp*W(NO)(CH_2CMe_3-d_x)(Ph-h_5) (**5′-*d*$_x$**). During the rest of the thermolysis, the signals for the starting material isotopomers decrease, while those of the products grow in, with no new signals being evident in the spectrum even after 90 h.[16]

All of the above results are consistent with the intermediacy of σ-neopentane complexes, as shown in Scheme 3. α-D abstraction from **1-*d*$_4$** generates two types of σ-neopentane alkylidene complexes via exchange of σ(C−H) and σ(C−D) bonds. Elimination of neopentane from either σ-complex leads to **A-*d*$_1$**, while reversion of the abstraction leads to the re-formation of **1-*d*$_4$** or to the formation of its H/D scrambled isotopomer, Cp*W(NO)($CH_{syn}DCMe_3$)(CH_2CMe_3-d_3) (**1′**). A second abstraction event from **1′** forms either **A-*d*$_1$** or **A′-*d*$_3$**, depending on which neopentyl ligand undergoes C−H bond cleavage. Thus, upon neopentane elimination, neopentane-d_1 and -d_3 are generated as well as the C−H activation products of **A-*d*$_1$** and **A′-*d*$_3$**. After one or more additional generations of σ-neopentane complexes without neopentane elimination, other starting material isotopomers are produced from **1′** in which the deuterium label is scrambled into the other positions of the neopentyl ligands. Upon elimination, these isotopomers can generate neopentane-d_4, neopentane-d_2, and neopentane-d_0, as well as additional α-H alkylidene intermediates **A′-*d*$_0$**, **A′-*d*$_1$**, **A′-*d*$_2$**, and **A′-*d*$_4$**, which contain 0, 1, 2, or 4 deuterium atoms in the ^{t}Bu group. However, even after repeated H/D exchange events, the formation of intermediates **A-*d*$_1$** and **A′-*d*$_3$**, and to a lesser extent **A′-*d*$_1$**, remains statistically dominant. Thus, the average number of deuterium atoms incorporated into the *tert*-butyl group remains close to three, while neopentane-d_3 and neopentane-d_1 are the dominant isotopomer byproducts, as indeed is observed experimentally.[17]

Other mechanisms for the observed H/D exchange in the neopentyl ligands which are not on the reaction

(15) The small negative values assigned to neopentane-d_0 are likely due to a combination of the assumptions made in the calculations (see Experimental Section) and the uncertainties in the average mass spectral intensities.

(16) Protio-phenyl complexes **5-*d*$_1$** and **5′-*d*$_x$** are sufficiently unstable toward β-H elimination of a second equivalent of neopentane under these conditions that the analysis of the neopentane isotopomer distribution from this reaction could not be included in Tables 1 and 2. See ref 6b for details.

Scheme 3

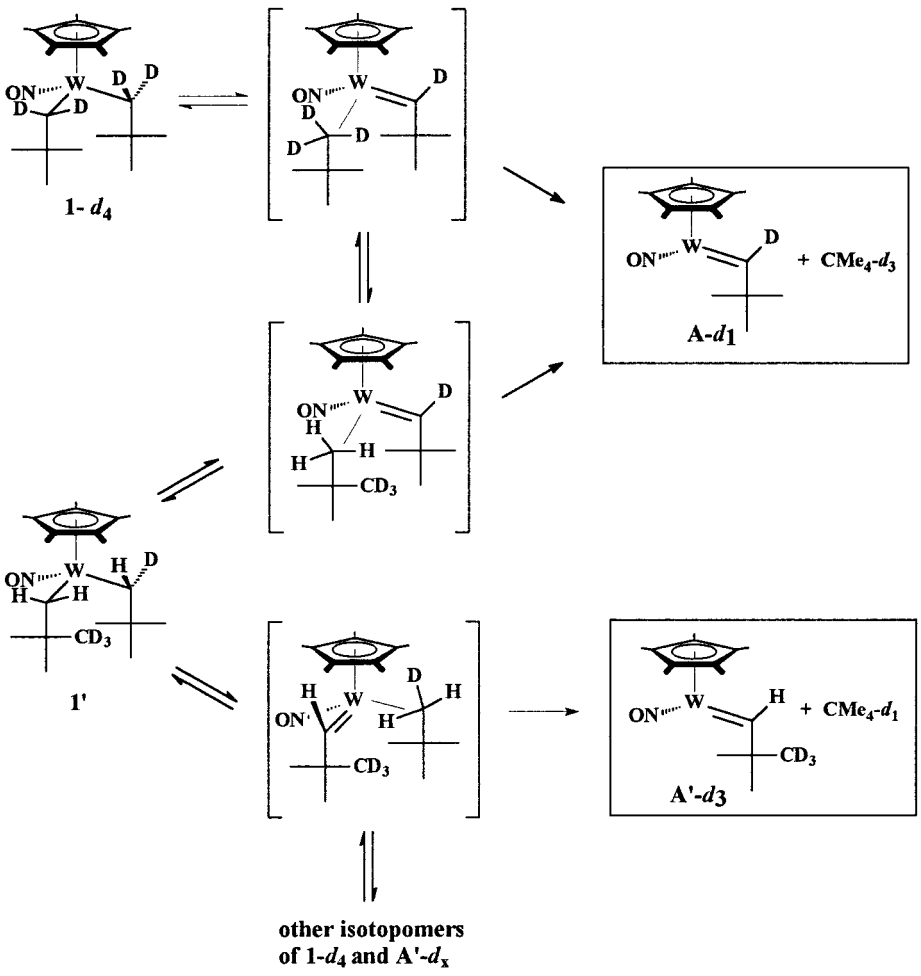

coordinate for formation of the alkylidene complex **A** can be discounted. For example, the lack of deuterium incorporation into the Cp* methyl groups of the starting material isotopomers rules out H/D exchange via reversible formation of tucked-in Cp* σ-neopentane complexes. Likewise, H/D exchange via reversible formation of metallacyclobutane σ-neopentane intermediates by γ-H abstraction would generate neopentane-d_3 and neopentane-d_2 as the principal byproducts. Finally, it is possible that the H/D exchange is a bimetallic rather than a monometallic intramolecular process.[12a,18] However, the thermolysis of **1-*d*$_4$** in benzene-d_6 at 70 °C at two different concentrations (15 mM and 75 mM) does not show any significant concentration effects on the rate of H/D exchange or product formation over the course of the reaction.

II. Reaction Coordinate for the Activation of Hydrocarbon Substrates by A and B. (a) Aliphatic Substrates. The results of part I clearly indicate that σ-neopentane complexes are intermediates during the formation of the reactive alkylidene species. By the principle of microscopic reversibility, σ-alkane complexes must be present in the activation of aliphatic C−H bonds by **A** and **B**. However, two limiting and fundamentally different qualitative reaction coordinates can be drawn for the activation of a generic alkane substrate, as shown in parts a and b of Figure 2. In both cases, the energies of the intermediate σ-complexes are comparable to each other but less than that of the reactive 16e alkylidene complex. In addition, the energy barriers for C−H bond scission from the σ-complexes are comparable to that for alkane dissociation to form the alkylidene complex. These features are consistent with the calculations by Poli and Smith, as well as the observed competitiveness of H/D exchange with product formation in the thermolyses of **1-*d*$_4$**.

Parts a and b of Figure 2 do differ, however, in the relative heights of the C−H bond scission energy barriers (i.e. $\Delta G^{\ddagger}_1$ and $\Delta G^{\ddagger}_4$ vs $\Delta G^{\ddagger}_2$ and $\Delta G^{\ddagger}_3$) and as such are fundamentally different in terms of the factors influencing alkane activation. Fortunately, the inter-

(17) The thermal decomposition of **1-*d*$_4$** has been previously monitored by UV−visible absorbance spectroscopy, and a first-order process was observed with a k_{obs} value of [2.01(1)] × 10^{-4} s^{-1} at 91 °C (R^2 = 0.9989).[6b] Without evidence of the H/D exchange process from this methodology, this k_{obs} value was equated to the rate constant for α-D elimination of neopentane ($k_{elim}(D_{syn})$) for pure **1-*d*$_4$**, and the α-H(D) isotope effect for neopentane elimination was reported as 2.4(2) (91 °C). In light of the results described in this section, it is now apparent that the thermal decomposition of **1-*d*$_4$** involves both direct elimination of neopentane from **1-*d*$_4$** as well as H/D exchange to H_{syn} isotopomers which intrinsically eliminate neopentane faster than **1-*d*$_4$**. In other words, the measured k_{obs} value is in fact a composite of the first-order rate constants for direct neopentane elimination from **1-*d*$_4$** ($k_{elim}(D_{syn})$) as well as for elimination from its H_{syn} isotopomers ($k_{elim}(H_{syn})$). Thus, the actual value of $k_{elim}(D_{syn})$ for pure **1-*d*$_4$** is likely less than 2.0 × 10^{-4} s^{-1} at 91 °C and the value of 2.4 is an underestimation of the true isotope effect for α-H neopentane elimination in this system.

(18) Booij, M.; Deelman, B.-J.; Duchateau, R.; Postma, D. S.; Meetsma, A.; Teuben, J. H. *Organometallics* **1993**, *12*, 3531−3540.

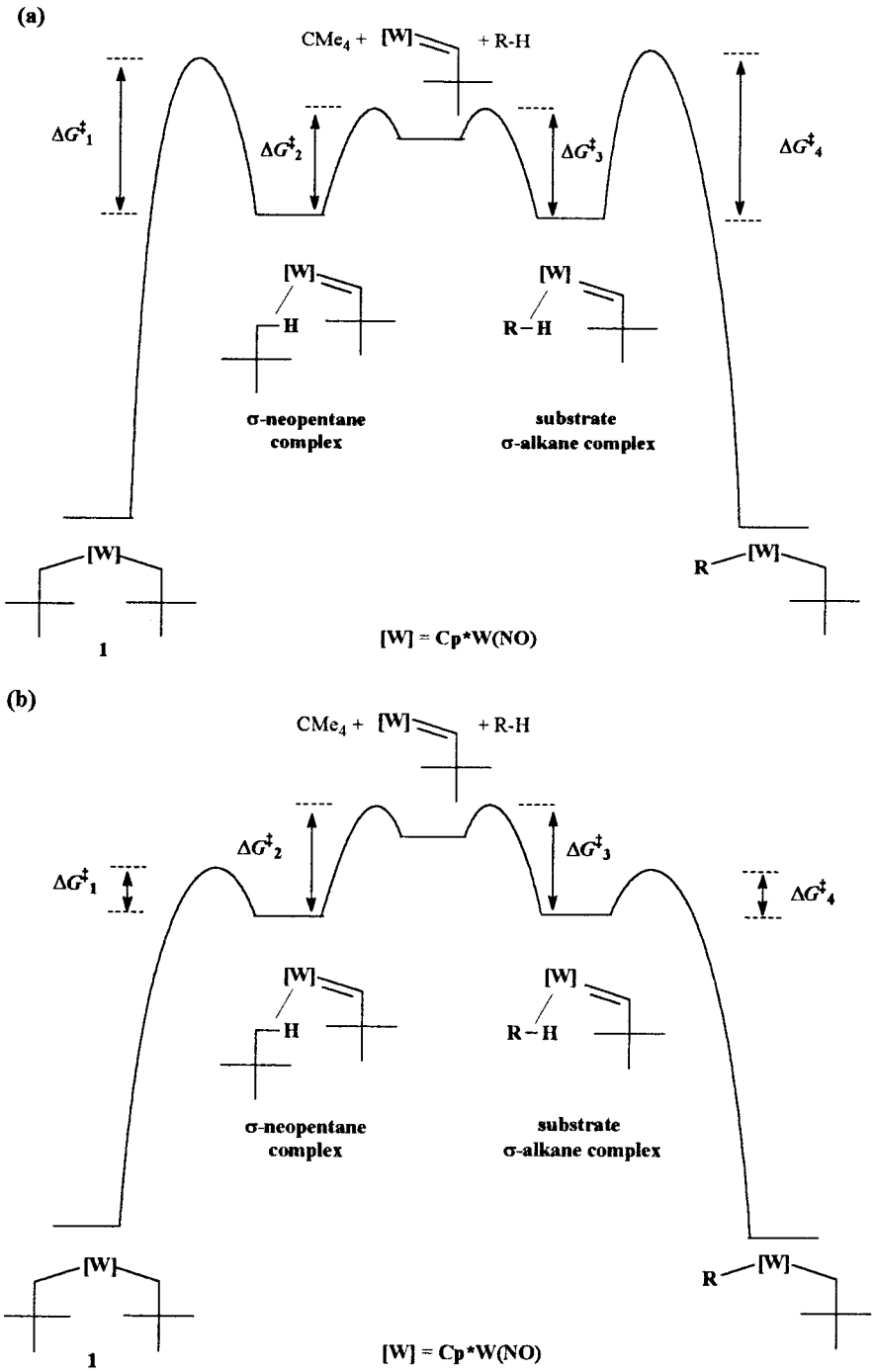

Figure 2. Possible qualitative potential energy surfaces for activation of an alkane substrate (R−H), using complex **1** and intermediate **A** as illustrative examples.

molecular isotope effect for the activation of tetramethylsilane provides a clear indication as to which of the two surfaces is the most viable.

The thermolysis of **1** in a 1:1 molar mixture of tetramethylsilane-h_{12} and tetramethylsilane-d_{12} (70 °C, 40 h) results in the formation of C−H and C−D activation products Cp*W(NO)(CH_2CMe_3)(CH_2SiMe_3) (**4-d_0**) and Cp*W(NO)($CHD_{syn}CMe_3$)(CD_2SiMe_3-d_9) (**4-d_2**) in a 1.07(4):1 ratio (eq 3, 95% CI).

The activation of tetramethylsilane has been shown to be irreversible under these conditions.[6b,19] Therefore, the observed product distribution represents the intermolecular kinetic isotope effect for aliphatic sp^3 C−H vs C−D bond activation by **A**. The near-unity KIE value indicates that **A** exhibits little preference for activating protio over deuterio substrates. This is clearly inconsistent with the reaction coordinate in Figure 2a, in which activation of the protio substrate would be significantly favored due to the rate-determining substrate C−H bond scission step and the corresponding preequilibrium of protio and deuterio coordinated substrates.[20] On the other hand, the experimental data can

(19) Note that activation now refers to both coordination of the substrate and cleavage of the C−H bonds. For irreversible activations, only the coordinate step need be irreversible for the substrate to be nonlabile once activated.

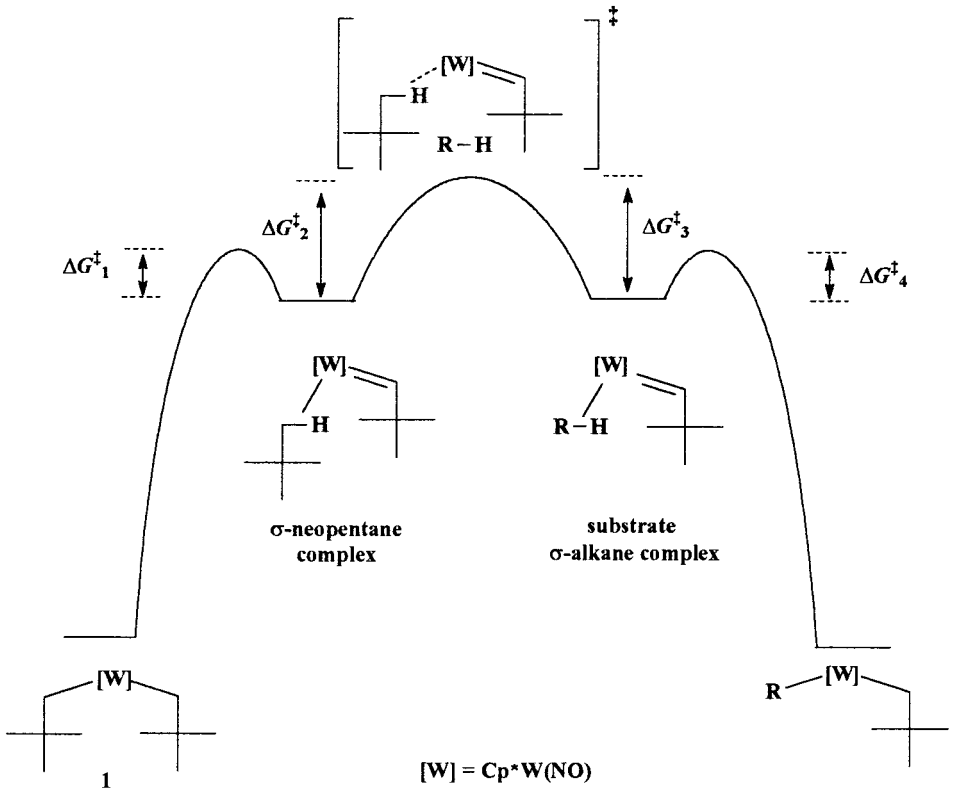

Figure 3. Alternative qualitative potential energy surfaces for activation of an alkane substrate (R−H) by an interchange-dissociative mechanism, featuring the σ-neopentane complex of **A** as the reactive alkylidene complex.

be fitted to Figure 2b. In this instance, the energy barrier to C−H bond scission from the substrate σ-complex is smaller than that for reversion back to the 16e

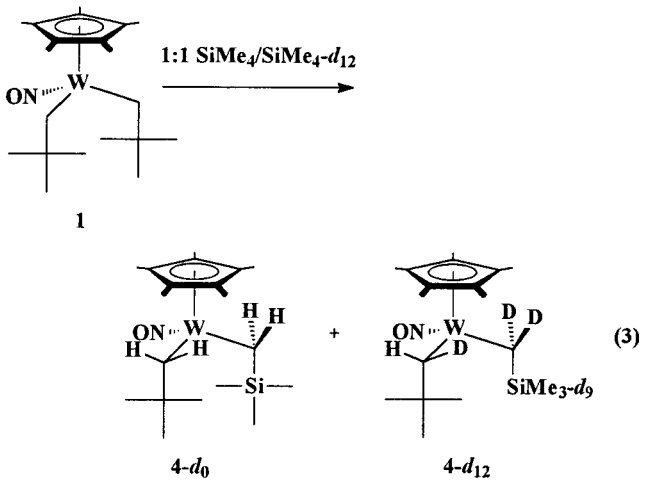

alkylidene complex. Thus, once a substrate is coordinated, the activation of the C−H (C−D) bond is faster than exchange with the solvent. Moreover, providing that there is little difference in the energetics of formation of the C−H vs C−D σ-complexes, the KIE for aliphatic C−H (C−D) bond activation will be small. A similar reaction coordinate has been presented to account for small intermolecular KIEs in the activation of alkanes by Cp*Ir(PMe_3) and related derivatives.[2]

It should be noted that another reaction coordinate fits the experimental data. In Figure 2b, the displacement of neopentane by the incoming alkane substrate occurs via a dissociative mechanism with alkylidene **A** existing as a discrete intermediate, as it has been assumed to be up to this point in the paper. Alternatively, the displacement of neopentane by the incoming alkane substrate may occur via an interchange-dissociative mechanism[21] in which the reactive alkylidene species is the preceding σ-neopentane complex (Figure 3). An important difference between the two reaction coordinates is the exact manner in which substrates are discriminated. In the first case, the intermolecular discrimination between substrates would correlate to the relative energy barriers for coordination of the C−H vs C−D sp^3 bonds to intermediate **A**. In the second instance, the intermolecular discrimination between substrates would originate in the relative transition-state energies for displacement of neopentane by substrate C−H and C−D bonds in the preceding σ-neopentane complex of **A**.[22]

Intuitively, the intimate-dissociative mechanism seems more likely, given that energy barriers to solvation of

(20) For examples in which C−H bond scission is rate-limiting and the intermolecular KIEs are significantly large, see: (a) Reference 4. (b) Jiang, Q.; Pestana, D. C.; Carroll, P. J.; Berry, D. H. *Organometallics* **1994**, *13*, 3679−3691. (c) Watson, P. L. *J. Am. Chem. Soc.* **1983**, *105*, 6491−6493.

(21) For a good illustration of the differences between these mechanisms, see: Cotton, F. A.; Wilkinson, G.; Gaus, P. L. *Basic Inorganic Chemistry*, 2nd ed.; Wiley: Toronto, 1987; pp 176−179.

(22) The other two possible mechanisms for exchange of neopentane for substrate, namely associative and interchange-associative mechanisms, can be ruled out. Both associative and intimate-associative mechanisms would require association of the substrate with the metal center prior to neopentane dissociation. However, this is not likely given the 18e nature of the σ-neopentane alkylidene complexes. Moreover, the rate constants for the thermolysis of **1** and **2**,[6b] and the degree of H/D exchange in **1-d_4**, do not show any significant solvent effects, which would be expected if the solvent is involved in the displacement of neopentane from the metal's coordination sphere.

the naked 16e intermediate **A** by the solvent molecules would not be expected. Yet, the existence of **A** as a discrete intermediate cannot be ruled out entirely either, as internal solvation by agostic interactions may be possible.[23] Thus, both reaction coordinates are viable, and the exact nature of the reactive alkylidene species and the manner in which substrates are discriminated between cannot be conclusively determined. Either way, however, the discrimination between substrates occurs upon coordination of the substrate to the metal center in the alkylidene fragments **A** and **B** (either as discrete complexes or within the σ-neopentane complex of **A** and **B**) and not upon cleavage of the substrate C−H (C−D) bonds. Note that, for simplicity, the reactive alkylidene fragments will continue to be regarded as the alkylidene complexes **A** and **B** for the duration of this paper.

(b) Arene Substrates. Intermolecular KIEs have also been determined for the activation of arene substrates by **A** and **B**. The thermolysis of **1** in a 1:1 molar mixture of benzene and benzene-d_6 at 70 °C for 40 h generates a product mixture of Cp*W(NO)(CH_2CMe_3)(C_6H_5) (**5-*d*$_0$**) and Cp*W(NO)($CHD_{syn}CMe_3$)(C_6D_5) (**5-*d*$_6$**) in a 1.03(5):1 ratio (95% CI, eq 4). Likewise, the

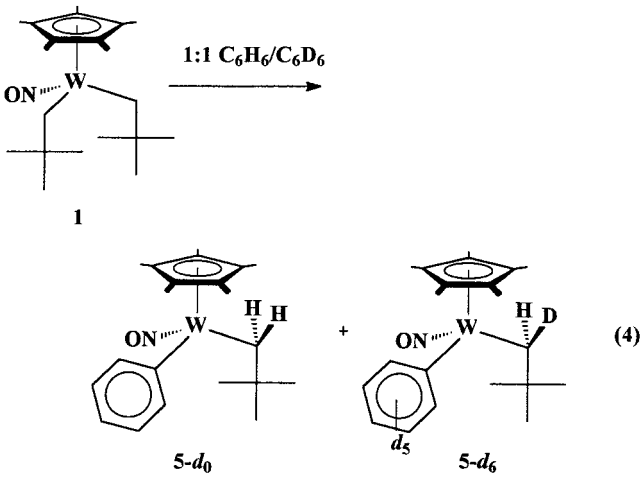

(4)

thermolysis of **2** under identical conditions generates a mixture of Cp*W(NO)($CH_2C_6H_5$)(C_6H_5) (**6-*d*$_0$**) and Cp*W(NO)($CHD_{syn}C_6H_5$)(C_6D_5) (**6-*d*$_6$**) in a 1.17(19):1 ratio. Benzene activation is irreversible under these conditions;[6b] therefore, these ratios represent the KIEs for aromatic sp^2 C−H vs C−D bond activation for **A** and **B**, respectively. The near-unity values once again indicate that C−H (C−D) addition to the M=C linkage is not rate limiting. Thus, the general shape of the energy surface depicted in Figure 2b and Figure 3 (i.e. $\Delta G^{\ddagger}_2 > \Delta G^{\ddagger}_1$ and $\Delta G^{\ddagger}_3 > \Delta G^{\ddagger}_4$) applies to the activation of benzene, and discrimination between substrates, either aliphatic or aromatic, lies with coordination of the substrate to the metal center. However, as illustrated in the next sections, there are some subtle, yet fundamental, differences between the reaction coordinates for sp^2 and sp^3 C−H bond activations.

III. Intramolecular Discrimination of the C−H Bonds within Toluene by A and B. The experimental work presented in parts I and II provides us with a general picture of the reaction coordinate for the chemistry derived from **1** and **2** and reveals that the coordination of the substrate to the metal center in **A** and **B** is the origin of discrimination *between* substrates. However, it remains to be discovered how the C−H bonds *within* a given substrate are discriminated. Typically, organometallic reagents lead to the preferential formation of the products of activation of the stronger C−H bond within a molecule.[1b] This appears to be the case for the activation of toluene by **A** and **B**, as well. Specifically, the aryl products of toluene activation, namely Cp*W(NO)(CH_2R)(C_6H_4Me) (R = CMe_3 for **A**, R = C_6H_5 for **B**), are formed preferentially over the benzyl products, Cp*W(NO)(CH_2R)($CH_2C_6H_5$) (aryl:benzyl = 4.3:1 (for **A**), 19:1 (for **B**)).[6b] Moreover, the respective aryl and benzyl products do not interchange when heated independently under thermolysis conditions, thereby indicating that the product distributions originate from the initial activation event mediated by **A** and **B**. Given the proven existence of substrate hydrocarbon complexes as intermediates prior to C−H bond scission, the discrimination between aryl and benzyl products of toluene may originate from either from the coordination of toluene to the metal center in **A** and **B** or from the subsequent aryl vs benzyl C−H bond addition to the M=C linkage of the intermediate hydrocarbon complexes. The true origin of the observed aryl vs benzyl product selectivity can be identified by first investigating another mechanistic aspect of toluene activation, specifically the origin of the distribution of regioisomeric aryl products.

(a) Reversibility of Aromatic sp^2 C−H Bond Activation. As described in the original report of toluene activation by **A** and **B**,[6b] the aryl products derived from **1** and **2** are subdivided into regioisomers (meta:para:ortho = 47:33:1 for **A**, meta:para = 1.97(11):1 for **B**, ortho isomer not observed). Furthermore, it was discovered that the regioisomeric product distributions are in thermodynamic equilibrium under the thermolysis conditions. This is demonstrated by the rapid intramolecular isomerization of ortho aryl isomers to the meta and para isomers, where the rate constants for the isomerization are an order of magnitude larger than the rate constants for alkylidene formation from **1** and **2** at 70 °C (i.e. $k_{isom} = 6.7 \times 10^{-4}$ s^{-1} for Cp*W(NO)(CH_2CMe_3)(C_6H_4-2-Me), $k_{isom} = 1.9 \times 10^{-4}$ s^{-1} for Cp*W(NO)($CH_2C_6H_5$)(C_6H_4-2-Me) vs $k_{elim} = 5 \times 10^{-5}$ for **1** and **2**). To isomerize, the aryl products must be undergoing a rapid intramolecular H transfer process via an unobserved intermediate. An intriguing possibility is that the unobserved intermediate is the same hydrocarbon complex involved in the initial coordination and activation of toluene. In other words, aromatic sp^2 C−H bond scission may be a reversible process.[24] There are several precedents in other C−H activation systems in which reversible formation of the hydrocarbon complex intermediates on the C−H activation reaction coordinate has been invoked to account for thermal rearrangements of activated products.[25,26] However, in this instance, several other intermediates could conceivably be involved in the intramolecular H-atom transfer, including tucked-in Cp*, metallacyclic, or aryne intermediates.

(23) Schaller, C. P.; Cummins, C. C.; Wolczanski, P. T. *J. Am. Chem. Soc.* **1996**, *118*, 591−611.

(24) Note that "reversible C−H bond scission" refers only to the C−H bond cleavage event, not to the overall activation process, which represents both substrate coordination and cleavage of a substrate C−H bond.

To elucidate the mechanism operative in the aryl ligand regioisomerizations, the labeled complex Cp*W(NO)(CH_2CMe_3)(C_6D_5) (**5-*d*$_5$**) has been thermolyzed in C_6D_6 and CD_2Cl_2 at 70 °C. Monitoring the thermolyses by ^{1}H NMR spectroscopy over 5 h reveals a rapid, exclusive, and concomitant exchange of hydrogen and deuterium between the synclinal methylene position of the neopentyl ligand and all three aromatic positions of the phenyl ligand to yield Cp*W(NO)($CHD_{syn}CMe_3$)($C_6D_4H_1$) (**5′-*d*$_5$**) (eq 5). The rate of conversion is independent of the solvent, and free benzene is not detected in the experiment conducted in CD_2Cl_2. A nonlinear least-squares analysis of the data from the reaction in CD_2Cl_2 using an exponential approach to equilibrium kinetic model yields a calculated k_{obs} value of [3.6(2)] × 10^{-4} s^{-1} (see the Supporting Information for details). This corresponds to rate constants of 3×10^{-4} s^{-1} for H transfer to the aryl ligand and 9×10^{-5} s^{-1} for D transfer to the aryl ligand. The calculated K_{eq} value of 3.0(3) for H incorporation into the aromatic region is less than the statistical K_{eq} value of 5, consistent with the preferential association of deuterium with the stronger aryl bond.

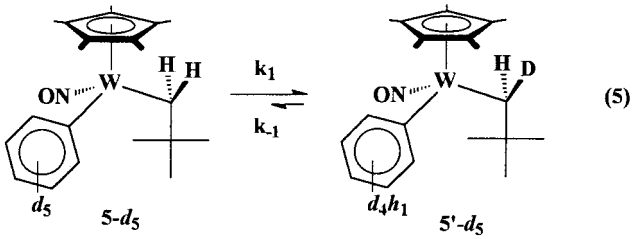

(5)

The rapid and exclusive H/D exchange between the phenyl ring and the synclinal methylene position, and the lack of incorporation of deuterium into any other positions of **5′** even on prolonged thermolysis (>40 h), are only consistent with reversible aromatic sp^2 bond C−H (C−D) cleavage, as illustrated in Scheme 4. Rapid interconversion of the intermediate arene complex to a different rotamer will result in aryl ligand isomerization upon readdition of the C−H bond across the M=C linkage.

An unresolved issue regarding this process is the exact nature of the arene complex. As shown in Scheme 4, one of two different arene complexes may be involved: an η^2 (sp^2-C,H) methylbenzene σ-complex (herein referred to as a σ-arene complex) or a π-arene complex.[11h] In other systems, the comparison of inter- and intramolecular kinetic isotope effects in benzene activation has been used successfully to distinguish between these two types of intermediates. For example, the intermolecular kinetic isotope effect for activation of molar mixtures of benzene/benzene-d_6 by Cp*Rh(PMe_3) is 1.0, while the intramolecular kinetic isotope effect for thermolysis in 1,3,5-benzene-d_3 is significantly larger at 1.4.[11b] The unity value for the intermolecular KIE and the difference in the two KIE values suggests that the C−H (C−D) bond is not involved in the substrate coordination step and thus supports the formation of a π-arene intermediate rather than a σ-arene intermediate in the Rh system. It would seem appropriate to apply a similar comparison of inter- and intramolecular KIEs to this system to determine the type of arene intermediates involved in alkylidene-mediated C−H activation. However, the usefulness of the comparison is obviated by the fact that the measured intramolecular isotope effect will be thermodynamic and not kinetic in nature, due to the rapid intramolecular H/D exchange between the aryl and methylene positions of the ligands under the requisite thermolytic conditions. In other words, the product ratios obtained from the thermolysis of **1** or **2** in 1,3,5-benzene-d_3 (70 °C, 40 h) would have no relation to the determination of the nature of the intermediate. An argument could be made that the near-unity intermolecular KIE values measured from the thermolysis of **1** and **2** in benzene/benzene-d_6 support the formation of π-arene intermediates. Yet, the intermolecular KIE for the activation of the molar mixture of tetramethysilane-h_{12} and tetramethysilane-d_{12} by **A** is also near unity, even though the C−H (C−D) bond must be involved in the substrate coordination in this instance. Clearly, neither arene coordination mode can be ruled out and the nature of the intermediate formed during benzene activation cannot be resolved by experimental methods in this instance.

Scheme 4

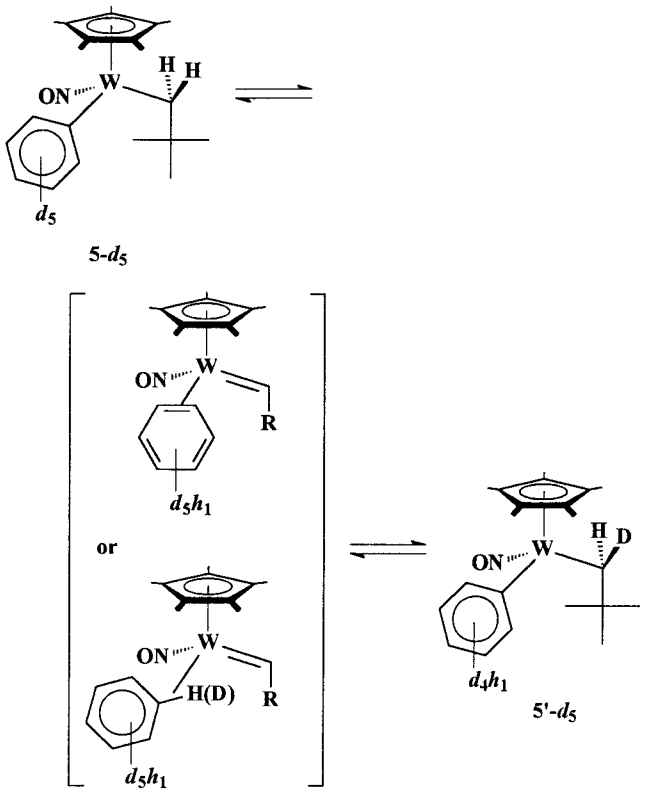

The cleavage of aromatic sp^2 C−H bonds appears to be reversible in the corresponding benzyl aryl complexes as well. Thermolysis of Cp*W(NO)($CH_2C_6H_5$)(C_6D_5) (**6-*d*$_5$**) in C_6D_6 at 70 °C results in exclusive synclinal

(25) (a) Feher, F. J.; Jones, W. D. *J. Am. Chem. Soc.* **1984**, *106*, 1650−1663. (b) Chin, R. M.; Dong, L.; Duckett, S. B.; Partridge, M. G.; Jones, W. D.; Perutz, R. N. *J. Am. Chem. Soc.* **1993**, *115*, 7685−7695. (c) Sweet, J. R.; Graham, W. A. G. *J. Am. Chem. Soc.* **1983**, *105*, 304−306.

(26) (a) Erker, G. *J. Organomet. Chem.* **1977**, *134*, 189−202. (b) Debad, J. D.; Legzdins, P.; Lumb, S. A.; Rettig, S. J.; Batchelor, R. J.; Einstein, F. W. B. *Organometallics* **1999**, *18*, 3414−3428. (c) Price, R. T.; Andersen, R. A.; Muetterities, E. L. *J. Organmet. Chem.* **1989**, *376*, 407−417.

methylene deuterium incorporation to yield Cp*W(NO)-($CHD_{syn}C_6H_5$)($C_6D_4H_1$) (**6′-*d*$_5$**) (eq 6).[27] Quantitative

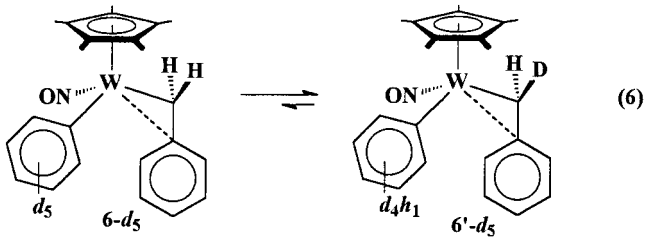

(6)

analysis of the exchange process in this case was prevented by the presence of overlapping resonances from contaminants in the original sample of **6-*d*$_5$** (see the Experimental Section). However, the initial rate of the exchange of **6-*d*$_5$** does appear to be qualitatively slower than that of **5-*d*$_5$**, a feature also seen in the isomerization of the related benzyl *o*-tolyl and neopentyl *o*-tolyl complexes (vide supra). A rationale for the difference in rates can be proposed on the basis of the mechanism in Scheme 4. The Cp′M(NO)(R)(R′) (Cp′ = Cp, Cp*; M = Mo, W; R = benzyl; R′ = alkyl, aryl, benzyl) complexes such as **6-*d*$_5$** possess a stabilizing η^2-benzyl interaction in the ground state.[6b,28] The aryl ligand isomerization and H/D exchange processes in the benzyl aryl complexes require the loss of the η^2 interaction prior to aryl C−H (C−D) bond cleavage and intramolecular H(D) transfer. The additional energy needed for the geometric change would increase the overall energy barrier for the transfer and thus slow the rates of H/D exchange and aryl ligand isomerization.

(b) Aryl vs Benzyl Product Selectivity Revisited. The reversibility of aryl C−H bond cleavage resolves the mechanism by which the aryl vs benzyl product discrimination arises from **A** and **B**. As discussed previously, there are only two possible points at which the discrimination between aryl and benzyl products can occur in the activation process: upon coordination of the substrate or upon cleavage of the C−H bond. The latter scenario can now be ruled out. In this instance, discrimination between the aryl and benzyl products would have to arise from the relative energy barriers associated with aryl vs benzyl C−H bond cleavage from a common hydrocarbon intermediate (e.g., a π-arene complex) or from π- and/or σ- complexes that undergo rapid exchange. However, the rapid reversibility of aromatic sp^2 C−H bond cleavage means that the π- or σ-arene complex that is involved in aryl ligand isomerization should lead to the formation of the corresponding benzyl products during the thermolyses of the *o*-tolyl products in toluene, in addition to the meta and para regioisomers. This scenario is clearly inconsistent with the observed experimental results.

The point of discrimination between aryl and benzyl products must therefore be in the coordination of the substrate to **A** and **B**. However, for these products to be formed independently by such a mechanism, the reaction coordinate for the activation of toluene must satisfy several conditions. First, *two distinct* types of hydrocarbon complexes must be formed for the pathways leading to aryl and benzyl products, either a π-arene or a σ-arene for aryl product formation and a η^2(sp^3-*C*,*H*)-phenylmethane σ-complex for benzyl product formation.[29] In addition, these two types of hydrocarbon complexes must not interconvert once formed, either by intramolecular isomerization or dissociation of toluene. Finally, the pathway leading to the π-arene/σ-arene complex must be kinetically preferred over that leading to the σ-phenylmethane complex, while the transition state energy for sp^2 C−H bond scission is small enough to permit rapid, reversible aryl ligand isomerization. Only if these four conditions are satisfied can the aryl and benzyl products form independently while rapid and reversible sp^2 C−H bond scission occurs.

The implied reaction coordinate for toluene activation by the reactive alkylidene complexes **A** and **B** is thus shown in Figure 4. Note that it is assumed that π-arene complexes are formed instead of σ-arene complexes along the pathway to formation of the aryl products (vide infra). Key features of Figure 4 are as follows.

(1) π-Arene coordination is kinetically preferred over σ-phenylmethane coordination (represented by $\Delta\Delta G^{\ddagger}$), in keeping with the observed preference for aryl products.

(2) From the π-arene complex, the energy barrier to sp^2 C−H bond scission is smaller than both the barrier to substrate dissociation and reversion back to the free alkylidene and the barrier to exchange with the σ-phenylmethane complex (represented by the dashed curve), in keeping with the lack of exchange between the hydrocarbon complexes.

(3) From the σ-phenylmethane complex, the energy barrier to sp^3 C−H bond scission is also lower than the energy barriers for dissociation and exchange.

Note that these last two features are also in keeping with the intermolecular KIEs measured for sp^2 and sp^3 C−H bond activations (vide supra), which indicate that substrate C−H bond scission is faster than substrate dissociation or hydrocarbon intermediate exchange. Note also that the observed lack of conversion of the benzyl product to its aryl isomers under thermolysis conditions may be assisted by the presence of the additional η^2-benzyl interaction that blocks access to the η^1-benzyl conformation required for reversion back to the σ-phenylmethane intermediate.

The alternative reaction coordinate for toluene activation by the σ-neopentane complexes of **A** and **B** is similar to that in Figure 4, except that the energy barriers for substrate coordination are larger than those for C−H bond scission. Also, since neopentane dissociation is rate-limiting and effectively irreversible, the π- or σ-arene and σ-phenylmethane complexes cannot exchange via by reversion back to the σ-neopentane complex. In both cases, the intramolecular aryl vs benzyl selectivity exhibited in the activation of toluene is driven by the faster formation of the π-arene complex over the σ-phenylmethane complex. Thus, the intrinsic strengths of the C−H bonds do not appear to be significant factors

(27) The corresponding incorporation of H into the phenyl region is obscured by signals for the aryl protons of the benzyl ligand.

(28) (a) Legzdins, P.; Jones, R. H.; Phillips, E. C.; Yee, V. C.; Trotter, J.; Einstein, F. W. B. *Organometallics* **1991**, *10*, 986−1002. (b) Dryden, N. H.; Legzdins, P.; Trotter, J.; Yee, V. C. *Organometallics* **1991**, *10*, 2857−2870.

(29) Herein, the two types of σ-complexes for toluene will be distinguished as the σ-arene complex for the η^2(sp^2-*C*,*H*)-methylbenzene coordination mode and the σ-phenylmethane complex for the η^2-(sp^3-*C*,*H*)-phenylmethane coordination mode.

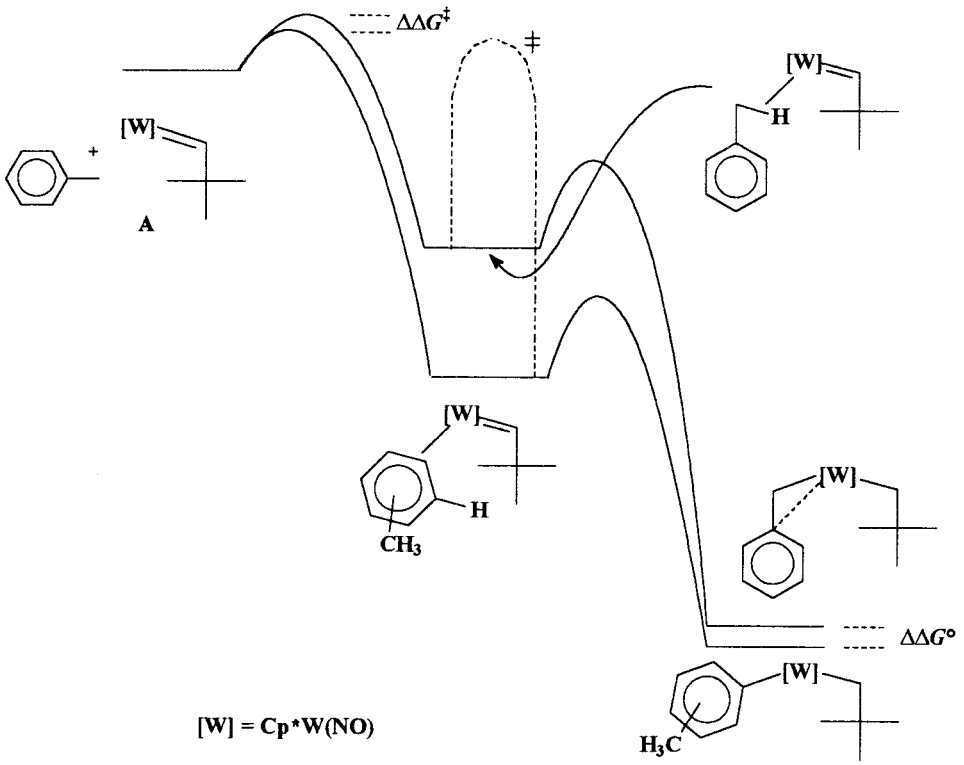

Figure 4. Qualitative depiction of the proposed free energy vs reaction coordinate diagram for the activation of toluene, using intermediate **A** as the reactive alkylidene species.

in governing product selectivity in this instance, and the fact that the stronger aryl bonds are preferentially activated is simply due to the link between preferential π-arene complex formation and aromatic sp^2 C−H bond cleavage.

IV. Theoretical Investigations into Toluene Activation by A and B. To substantiate this interpretation of the toluene activation reaction coordinate, rudimentary DFT calculations have been conducted on the coordination and activation of toluene by an alkylidene complex. The calculations have been conducted in the manner employed by Poli and Smith, using CpW(NO)-(=CH_2) (**C**) as a simplified version of the alkylidene complexes **A** and **B** and the LANL2DZ basis set to minimize computational expense. Optimized geometries and the corresponding gas-phase free energies have been determined for various species involved in the activation process, as discussed below.

(a) Benzyl and Aryl Products of Toluene C−H Activation. The optimized geometry of the benzyl product of toluene activation by **C**, namely CpW(NO)-(CH_3)($CH_2C_6H_5$), is shown in Figure 5a. Most notably, the benzyl ligand is coordinated in the expected η^2 fashion. The optimized geometries of the regioisomeric aryl products have also been determined, and a representative structure is shown in Figure 5b (see the Supporting Information for pictures of all optimized complexes). A noteworthy feature of the aryl products is the distortion of one of the methyl C−H bonds (W−C−H(*) = 103.7° vs W−C−H = 113.9°), which is indicative of an α-agostic interaction with the metal center. Such interactions have recently been detected by neutron diffraction analysis and spectroscopic methods in related Cp′M(NO)(R)(R′) complexes (R = hydrocarbyl, R′ = hydrocarbyl, aryl, halide).[30]

(b) Intermediate Hydrocarbon Complexes. The placement of toluene in various orientations near the open coordination site of **C** results in two distinct classes of hydrocarbon complexes. Placement of one of the methyl C−H bonds close to the metal center in several orientations results in the $\eta^2(sp^3\text{-}C,H)$,σ-phenylmethane complex (**D**) upon geometry optimization (Figure 6a). Not surprisingly, the geometrical parameters of **D** are nearly identical with the corresponding σ-methane intermediate optimized by Poli and Smith and shown in Scheme 2.[8] Placement of toluene with the bulk of the arene ring being parallel to the NOW=CH_2 plane of **C** (i.e., face on) and away from the Cp* ring results in optimized structures of the type shown in Figure 6b, namely **E**. Likewise, initial geometries with the arene ring perpendicular to the NOW=CH_2 plane (i.e., edge on), or face on with the bulk of the arene ring close to the Cp ligand result in geometry optimizations to arene complexes of the type shown in Figure 6c (**E′**). Type **E** complexes are readily described as π-arene complexes, given the parallel arrangement of the arene ring and the W=CH_2 bond. At first glance, type **E′** complexes would appear to be bound in a σ-arene fashion through an sp^2 C−H bond, given the obtuse angles between the arene ring and the W=CH_2 bond and the close distance between the metal center and an aryl H atom. However, examination of the molecular orbitals of the para **E′** congener reveals that the bonding interaction between the metal center and the arene involves the π-orbitals of the aromatic ring and not the orbital of the closest sp^2 C−H bond. Thus, despite the different geometries, it appears that type **E′** complexes are also π-arene complexes and are interconvertible with type **E** com-

(30) Bau, R.; Mason, S. A.; Patrick, B. O.; Adams, C. S.; Sharp, W. B.; Legzdins, P. *Organometallics*, in press.

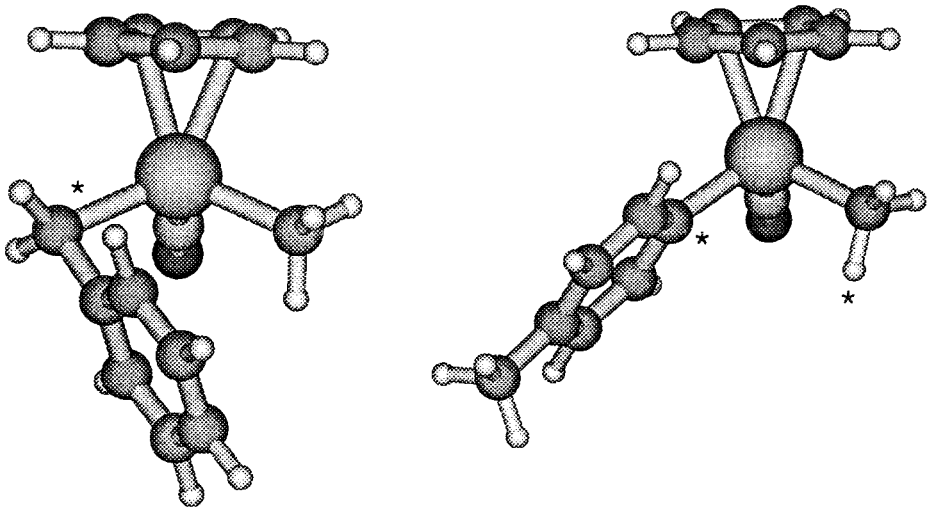

(a) W-CH_2 = 1.9705
W-CH_2 = 2.1723
W-C(*) = 2.1761
C(*)-C_{ipso} = 2.6237
W-C_{ipso} = 2.8313
C(*)-W-CH_2 = 121.5
W-C(*)-C_{ipso} = 89.2

(b) W-C(*) = 2.2625
W-C(*) = 2.1069
W-CH_2 = 2.1394
W-H(*) = 2.6311
H_2C-H(*) = 1.1045
HH(*)C-H = 1.0985
C(*)-W-CH_2 = 108.9
W-CH_2-H(*) = 103.7
W-CHH(*)-H = 113.9
H(*)-CH_2-W-C(*) = 33.0

Figure 5. Optimized geometries of (a) the benzyl product derived from sp^3 C−H bond activation of toluene and (b) the para aryl product derived from sp^2 C−H bond activation of toluene. In this instance, the asterisk denotes the C atoms of the new metal−carbon bond and the C−H agostic bond in (b).

plexes via simple rotation of the arene ring about the W−π bond. It can be inferred from these results that π-arene complexes are the reactive intermediates in the formation of the aryl products, rather than σ-arene complexes.

The orientation of the methyl group in toluene has some influence on the optimized geometries of the π-complexes **E** and **E′**. For the most part, steric interactions between the methyl group and the methylene linkage or Cp ring only induce mild geometric derivations from those shown in parts b and c of Figure 6. In some instances, however, these steric interactions are sufficient to prevent optimization of specific rotamers of both **E** and **E′** π-complexes.

(c) Transition States for Benzyl and Aryl C−H bond Cleavage. Transition states have been located for cleavage of both sp^3 and sp^2 C−H bonds. For sp^3 C−H bonds, the transition state is a logical geometric successor to the σ-phenylmethane complex **D** as the η^2-bound C−H bond of **D** is being cleaved (Figure 7a). It is very similar geometrically to the transition state for methane C−H bond scission shown in Scheme 2[8] and is best described as a metal-assisted 1,2-cis addition of C−H to the M=C linkage. For sp^2 C−H bonds, five different transition states were located for different orientations of the methyl group with respect to the activated bond. A representative structure for para aryl C−H bond activation is shown in Figure 7b. The transition states all possess very similar geometries about the atoms involved in the C−H bond addition and are geometrically quite similar to the metal-assisted early transition state for sp^3 C−H bond activation. One difference between the transition states for sp^2 and sp^3 C−H bond activations is that the incipient W−C bond from activation is significantly shorter for aryl activation (2.267 Å vs 2.396 Å). Finally, geometry optimization performed from representative sp^2 C−H bond activation transition states results in optimization to the respective **E′** π-arene complex as a local minimum. Thus, the calculated transition states and the hydrocarbon π-complexes **E** and **E′** lie on the same reaction coordinate, with no other intermediates lying between them. In other words, two distinct types of intermediates do indeed appear to lead to the aryl and benzyl products of toluene activation.

(d) Theoretical Reaction Coordinate For Toluene Activation. The relative gas-phase free energies for the products, intermediates, and transition states are collected in Tables 3−5. Figure 8 depicts the relative displacement of these species on the reaction coordinate for toluene activation.

The computed energetic data in Tables 3−5 and Figure 8 should be considered as semiquantitative, since the basis set employed contains no polarization and diffuse functions on tungsten and the ligand atoms.[31] Nevertheless, the calculations support the basic conclusion drawn from the experimental data: the C−H activation pathway leading to the aryl products through π-arene complexes is lower in energy than the pathway leading to the benzyl product via the σ-phenylmethane complex. Interestingly, the calculated potential energy barrier for the regioisomerization of the methyl *o*-tolyl complex CpW(NO)(CH_3)(C_6H_4-2-Me) is 32.8−33.7 kcal/

(31) Levine, I. N. *Quantum Chemistry*, 5th ed.; Prentice Hall: Upper Saddle River, NJ, 2000.

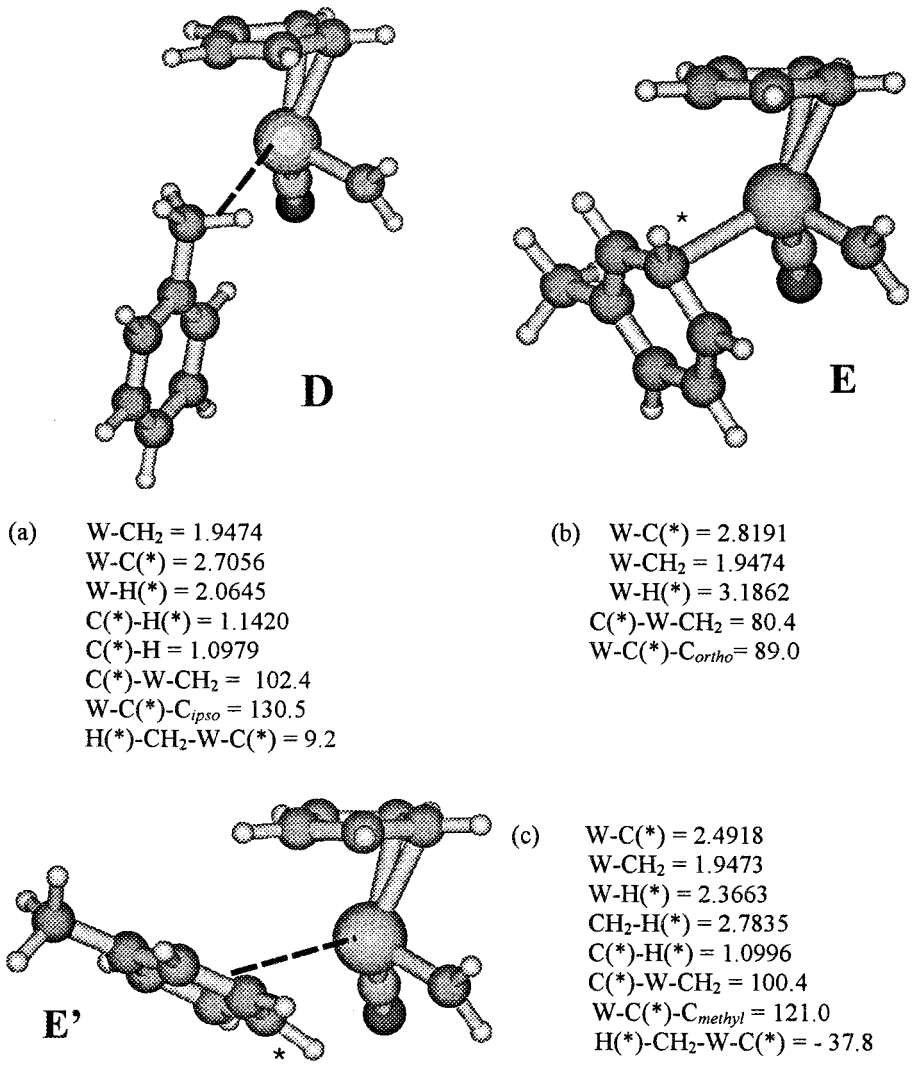

Figure 6. Optimized geometries and selected bond distances (Å) and angles (deg) of (a) the hydrocarbon complex **D**, (b) the representative (meta, anti) complex **E**, and (c) the para complex **E′**. In (b) and (c), the asterisk denotes the H and C atoms closest to the metal center.

mol (298 K), which is reasonably close to the free energy for isomerization of the related neopentyl *o*-tolyl complex, Cp*W(NO)(CH_2CMe_3)(C_6H_4-2-Me) (26 kcal/mol, 343 K), considering the limitations of the model system and the computational techniques employed.[32] Another notable feature is that the energies of the optimizable aryl regioisomers are very similar to that of the benzyl complex. This suggests that the well-documented stability of the formally 18e η^2-benzyl complexes Cp′M(NO)($CH_2C_6H_5$)(R′) as compared to their 16e aryl congeners[33] is a kinetic rather than a thermodynamic effect. A more detailed DFT investigation of the full reaction coordinate using more advanced theoretical methods to fully model both neopentylidene **A** and benzylidene **B** is required to confirm these observations and obtain quantitative theoretical data for the reaction coordinate.[31]

Table 3. Calculated Energies for the Aryl and Benzyl Products of Toluene C−H Bond Activation by C

complex	orientation of methyl group[a]	rel energy (kcal/mol)[b]
CpW(NO)(CH_3)($CH_2C_6H_5$)		3.7
CpW(NO)(CH_3)($C_6H_4CH_3$)	ortho, anti	3.6
	ortho, syn	4.7
	meta, syn	0.8
	para	0.0

[a] With respect to C(*) in part a or b of Figure 5 and the Cp−W bond. [b] With respect to *p*-CpW(NO)(CH_3)(C_6H_4-4-CH_3).

Epilogue

The experimental and theoretical studies presented here have greatly advanced our understanding of the C−H activation chemistry exhibited by this system. It is now apparent that hydrocarbon complexes are intermediates in the activation processes for both alkane and arene substrates. Moreover, the formation of these intermediates is intimately linked to the observed activation chemistry. Specifically, coordination of the substrate to the metal center, either in **A** and **B** as discrete intermediates or in σ-neopentane complexes of

(32) The difference may be due in part to the difference between gas-phase and solution-phase free energies, to the inflexible basis set employed, and to the limitations of the B3LYP DFT approach. However, the formations of methylidene analogues of neopentylidene complexes have been found to be energetically less favorable in both theoretical and experimental studies. For example, see: (a) Wu, Y.-D.; Peng, Z. H.; Xue, Z. *J. Am. Chem. Soc.* **1996**, *118*, 9772−9777. (b) Warren, T. H.; Schrock, R. R.; Davis, W. M. *J. Organomet. Chem.* **1998**, *569*, 125−137.

(33) Legzdins, P.; Veltheer, J. E. *Acc. Chem. Res.* **1993**, *26*, 41−48.

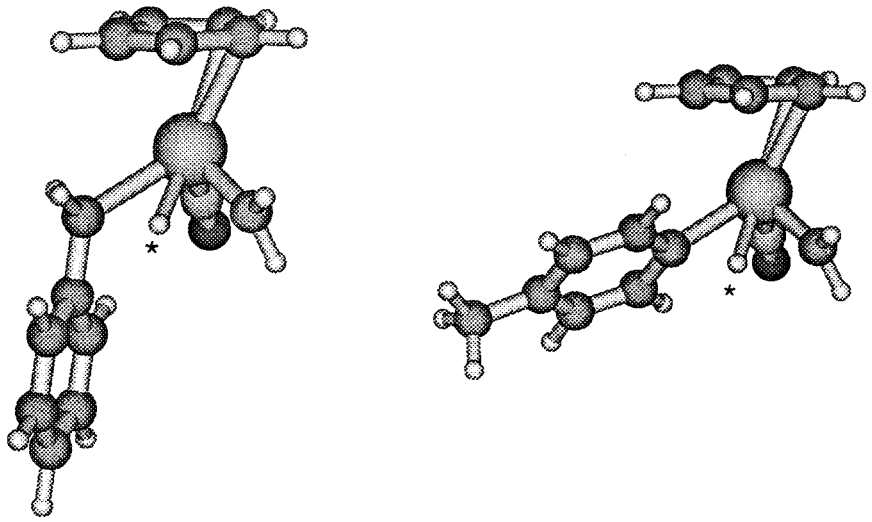

(a) W-CH_2 = 1.9705
W-C(*) = 2.3960
W-H(*) = 1.8018
C(*)-H(*) = 1.4747
H_2C-H(*) = 1.7156
C(*)-W-CH_2 = 91.8
C(*)-W-H(*) = 37.9
H_2C-W-H(*) = 53.9
W-C(*)-C_{ipso} = 127.0
H(*)-CH_2-W-C(*) = -1.3

(b) W-C(*) = 2.2625
W-CH_2 = 1.9827
W-H(*) = 1.8508
CH_2--H(*) = 1.6910
C(*)-H(*) = 1.4494
C(*)-W-CH_2 = 91.8
H(*)-W-C(*) = 52.1
H(*)-W-CH_2 = 39.7
H(*)-CH_2-W-C(*) = 3.0

Figure 7. Optimized geometries of the transition states for (a) sp^3 C−H bond activation and (b) para sp^2 C−H bond activation. In this instance, the asterisk denotes the H and C atoms of the C−H bond being cleaved.

Table 4. Calculated Energies for the Optimized Hydrocarbon Intermediates from Coordination of Toluene to Alkylidene Fragment C

complex	orientation of methyl group[a]	rel energy (kcal/mol)[b]
CpW(NO)(=CH_2)(H−$CH_2C_6H_5$) (**D**)		32.1
CpW(NO)(=CH_2)($C_6H_5CH_3$) (**E**)	meta, syn	23.6
	para	22.9
	meta, anti	24.2
	ortho, anti	24.7
CpW(NO)(=CH_2)($C_6H_5CH_3$) (**E′**)	ortho, syn	24.2
	meta, syn	24.2
	para	23.7
	ortho, anti	24.0

[a] Ortho, meta, and para are defined with respect to C(*)−H(*) in parts b and c of Figure 6, while synclinal and anticlinal are defined with respect to the W=CH_2 bond. [b] With respect to *p*-CpW(NO)(CH_3)(C_6H_4-4-CH_3).

Table 5. Calculated Energies for the Transition States Corresponding to Aryl and Benzyl Product Formation

complex	orientation of methyl group[a]	rel energy (kcal/mol)[b]
CpW(NO)(H_2C···H···$CH_2C_6H_5$)		41.8
CpW(NO)(H_2C···H···C_6H_4−CH_3)	ortho, anti	37.3
	ortho, syn	37.5
	meta, syn	33.0
	meta, anti	33.2
	para	32.7

[a] Defined with respect to C(*)−H(*) in Figure 7(b) and the Cp−W bond. [b] With respect to *p*-CpW(NO)(CH_3)(C_6H_4-4-CH_3).

A and **B**, is the discriminating step in both inter- and intramolecular C−H activation scenarios. In the activation of aromatic sp^2 C−H bonds, the formation of the intermediate π-arene complexes is reversible, thereby permitting thermal regioisomerizations to thermodynamic product distributions in instances where more than one aryl product is possible. In the case of toluene activation, the preferential coordination of the toluene substrate in the π-arene mode over the σ-phenylmethane mode directs the observed preferential formation of aryl products over benzyl products.

The fact that substrate coordination is the key step in the initial C−H bond activation event distinguishes these alkylidene complexes from other organometallic systems that operate by rate-determining C−H bond scission.[34] Interestingly, other C−H activating complexes that exhibit coordination-controlled selectivity include the classic thermally generated fragments Cp*M(PMe_3) (M = Ir, Rh). Given the extensive body of literature on these complexes and subsequent derivatives, the correlation between these systems and ours will be of great use in directing the development of our alkylidene complexes toward their ultimate application as selective C−H activating reagents for synthetic applications.

Experimental Section

General Methods. All reactions and subsequent manipulations were performed under anaerobic and anhydrous conditions. General procedures routinely employed in these laboratories have been described in detail previously.[35] Unless

(34) For some examples, see: (a) Schaller, C. P.; Wolczanski, P. T. *Inorg. Chem.* **1993**, *32*, 131−144. (b) Thompson, M. E.; Baxter, S. M.; Bulls, R.; Burger, B. J.; Nolan, M. C.; Santarsiero, B. D.; Schaefer, W. P.; Bercaw, J. E. *J. Am. Chem. Soc.* **1987**, *109*, 203−219. (c) Wang, C.; Ziller, J. W.; Flood, T. C. *J. Am. Chem. Soc.* **1995**, *117*, 1647−1648.

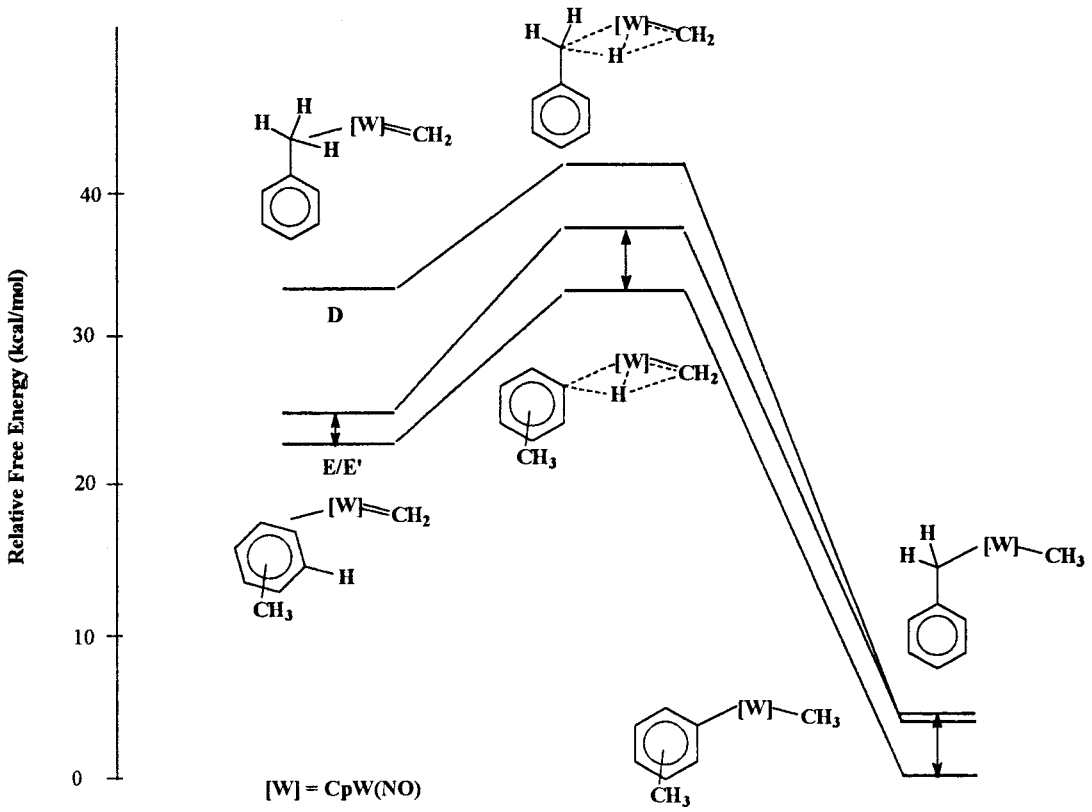

Figure 8. Free-energy profiles of the intermediates, transition states, and products of toluene activation by methylidene **C** as determined by DFT calculations.

otherwise stated, all chemicals were purchased from commercial suppliers and were used as received. Tetramethylsilane-d_{12} (99.8%CDN Isotopes) and benzene-d_6 (Cambridge) were distilled from Na or Na/benzophenone ketyl prior to use. Methylene chloride-d_2 and chloroform-*d* (Cambridge) were dried over activated 4 Å molecular sieves and vacuum-transferred as required. The $R_2Mg{\cdot}x$(dioxane) (R = $CH_2C_6H_4$-3-Me, C_6D_5, CX_2CMe_3; X = H, D) alkylating reagents[36,37] and the organometallic reagents Cp*W(NO)(CH_2CMe_3)Cl,[38] Cp*W(NO)(CH_2CMe_3)$_2$ [30] (**1**), and Cp*W(NO)($CH_2C_6H_5$)(CH_2-CMe_3) (**2**)[6b] were prepared according to published procedures. Cp*W(NO)($CH_2C_6H_5$)(Cl) was prepared by a modification of the reported procedure:[28b] a stoichiometric amount of 1.0 M HCl in Et_2O was used to effect protonolysis instead of an atmosphere of HCl gas. The labeled compounds Cp*W(NO)-(CD_2CMe_3)$_2$ (**1-*d*$_4$**), Cp*W(NO)(CH_2CMe_3)(C_6D_5) (**5-*d*$_5$**), and Cp*W(NO)($CH_2C_6H_5$)(C_6D_5) (**6-*d*$_5$**) were prepared by analogous metathetical methods from the appropriate chloride precursor and $R_2Mg{\cdot}x$(dioxane) reagent. Pertinent synthetic details and characterization data for these compounds are provided in the text below.

All IR samples were prepared as Nujol mulls sandwiched between NaCl plates and recorded on a ATI Mattson Genesis Series FT-IR spectrometer. NMR spectra were recorded at room temperature on Bruker AC 200, Varian XL 300, and Bruker WH-400, AV-400, and AMX 500 instruments. All chemical shifts are reported in ppm, and all coupling constants are reported in Hz. ^{1}H NMR spectra are referenced to the residual protio isotopomer present in a particular solvent, while ^{2}H{^{1}H} NMR spectra are referenced to C_6H_5D (7.15 ppm). ^{13}C NMR spectra are referenced to the natural-abundance carbon signal of the solvent employed. GC/MS analyses were performed on a Hewlett-Packard 6890 gas chromatograph with a HP-5MS column (30 M × 0.25 mm × 0.25 μm) and a 5973N mass-selective detector. Low-resolution mass spectra (EI, 70 eV, probe temperature 150 °C) were recorded by Mr. M. Lapawa and Ms. L. Madilao of the UBC mass spectrometry facility using a Kratos MS-50 spectrometer. Elemental analyses were performed by Mr. P. Borda of this department.

Preparation of Cp*W(NO)(CD_2CMe_3)$_2$ (1-*d*$_4$). The complex **1-*d*$_4$** was prepared in a manner analogous to **1** using (Me_3-CCD_2)$_2$Mg·*x*(dioxane), except that the pentane extract was filtered through Celite rather than alumina I.

^{1}H NMR (400 MHz, C_6D_6): δ 1.32 (s, 9H, CMe_3), 1.47 (s, 15H, C_5Me_5). ^{2}H{^{1}H} NMR (77 MHz, C_6H_6): δ − 1.51 (br s, D_{syn}), 2.69 (br s, D_{anti}). Anal. Calcd for $C_{20}H_{33}D_4NOW$: C, 48.49; H/D,[39] 7.53; N, 2.83. Found: C, 48.80; H/D, 7.41; N, 2.85.

Thermolyses of 1-*d*$_4$ in Tetramethylsilane, Benzene, and Benzene-*d*$_6$. A J. Young NMR tube was charged with **1-*d*$_4$** (12 mg, 0.024 mmol) and the appropriate solvent (0.8 mL). Two additional thermolyses were also conducted in benzene-d_6 at two different concentrations (6 and 30 mg in 0.80 mL of solvent), with hexamethyldisilane (2 mg, 0.014 mmol) added as an internal integration standard. The thermolyses were conducted in a VWR 1160A constant-temperature bath set at 70.0 °C. The tubes were periodically removed to record ^{1}H or ^{2}H{^{1}H} NMR spectra at ambient temperature. After 90 h, the organic volatiles were separated in vacuo and were analyzed by GC/MS. The organometallic residue was analyzed further

(35) Legzdins, P.; Rettig, S. J.; Ross, K. J.; Batchelor, R. J.; Einstein, F. W. B. *Organometallics* **1995**, *14*, 5579−5587.
(36) Dryden, N. H.; Legzdins, P.; Rettig, S. J.; Veltheer, J. E. *Organometallics* **1992**, *11*, 2583−2590.
(37) Legzdins, P.; Rettig, S. J.; Veltheer, J. E. *Organometallics* **1993**, *12*, 3575−3585.
(38) Debad, J. D.; Legzdins, P.; Batchelor, R. J.; Einstein, F. W. B. *Organometallics* **1993**, *12*, 2094−2102.

(39) Since the detection method used in the elemental analysis cannot distinguish between D_2O and H_2O, H/D abundances were calculated using 1 D = 1 H.

by ^{1}H or ^{2}H{^{1}H} NMR spectroscopy. Products were identified by comparison of the spectral data with those for the corresponding products of C−H and C−D activation from the thermolysis of **1** in protio and perdeuterio solvent (i.e. for tetramethylsilane, the data were compared to those exhibited by Cp*W(NO)(CH_2CMe_3)(CH_2SiMe_3) and Cp*W(NO)($CH_{syn}DCMe_3$)(CD_2SiMe_3-d_9).[6b]

From the thermolysis in tetramethylsilane: Cp*W(NO)($CH_{syn}DCMe_3$)(CH_2SiMe_3) (**4-d_1**) and Cp*W(NO)(CH_2CMe_3-d_x)(CH_2SiMe_3) (**4′-d_x**). ^{1}H NMR (400 MHz, C_6D_6): δ −2.16 (overlapping dd and s, Npt CH_{syn}H and Npt CH_{syn}D), −1.29 (dd, $^2J_{HH}$ = 12.0, $^4J_{HH}$ = 2.2, TMS CH_{syn}H), 0.42 (s, $SiMe_3$), 1.07 (d, $^2J_{HH}$ = 12.0, TMS CH_{anti}H), 1.35 (s, CMe_3), 1.53 (s, C_5Me_5), 3.28 (d, $^2J_{HH}$ = 12.8, Npt CH_{anti}H). ^{2}H{^{1}H} NMR (61 MHz, C_6H_6): δ 1.25 (br s, CMe_3-d_x), 3.23 (br s, CD_{anti}H). The intensity of the C$H_{anti}CMe_3$ signal of **4′-d_x** in the ^{1}H (C_6D_6) NMR spectrum was 48(2)% of the combined C$H_{syn}HSiMe_3$ doublets for **4-d_1** and **4′-d_x**, while the intensity of the ^{t}Bu resonance vs the Cp* resonance in the ^{1}H NMR spectrum was 85(2)% of the intensity for a fully protio ^{t}Bu moiety (0.66:1.00 or ∼9 H:15 H as in the case of Cp*W(NO)(CH_2CMe_3)(CH_2SiMe_3). The average number of H atoms per ^{t}Bu group is thus ((0.85 × 9) − (0.52 × 9))/0.48 or 6.2. Therefore, x in **4′-d_x** is approximately 2.8.

From the thermolysis in C_6D_6: Cp*W(NO)(CD_2CMe_3)(Ph-d_5) (**5-d_7**) and Cp*W(NO)($CHD_{syn}CMe_3$-d_x)(Ph-d_5) (**5′-d_y**). ^{1}H NMR (400 MHz, C_6D_6): δ 1.24 (s, CMe_3), 1.53 (s, C_5Me_5), 4.35 (br s, CH_{anti}D). ^{2}H{^{1}H} NMR (61 MHz, C_6H_6): δ −2.01 (br s, CD_{syn}D and CD_{syn}H), 1.18 (br s, CMe_3-d_x), 4.34 (br s, CD_{anti}D), 6.9−7.2 (Ph D).

From the thermolysis in C_6H_6: Cp*W(NO)($CH_{syn}DCMe_3$)(Ph-h_5) (**5-d_1**) and Cp*W(NO)(CH_2CMe_3-d_x)(Ph-h_5) (**5′-d_x**). ^{1}H NMR (400 MHz, C_6D_6): δ −2.06 (br s, CH_{syn}D), 1.26 (s, CMe_3), 1.54 (s, C_5Me_5), 4.49 (d, $^2J_{HH}$ = 11.8, CH_{anti}H), 7.10 (m, Ph H), 7.70 (d, $^3J_{HH}$ = 6.0, Ph H). ^{2}H{^{1}H} NMR (61 MHz, C_6H_6): δ 1.22 (br s, CMe_3-d_x), 4.50 (br s, CD_{anti}H).

GC/MS Analysis of Organic Volatiles. GC/MS spectra were recorded in triplicate using an 80 eV ionizing beam. Average intensities were determined for neopentane fragment peaks 57−61. The neopentane isotopomer composition of each sample was then deduced by matrix methods as described by Girolami and co-workers,[7c] using the experimental matrix coefficients for neopentane-d_0 to neopentane-d_3 under the assumption that all deuterium atoms reside on the same carbon. The coefficients for neopentane-d_4 were calculated assuming that $(CD_3)(CH_2D)C(CH_3)_2$ was the only isotopomer present.

Inter- and Intramolecular Competition Experiments. Intermolecular competition experiments were all conducted in a similar manner. A small reaction bomb was charged with **1** or **2** (12−15 mg), a stir bar, and 3 mL of a 1.0:1.0 (v/v) mixture of C_6H_6/C_6D_6 or ∼2 mL of a 1.0:1.0 (mol/mol) mixture of $SiMe_4$/$SiMe_4$-d_{12}. After the stirred mixtures were heated at 70(2) °C for 40 h in an oil bath, the solvent was removed in vacuo and a ^{1}H NMR (C_6D_6) spectrum was recorded. All products have been characterized previously.[6b] For reactions of **1**, the Cp*W(NO)(CH_2CMe_3)(C_6H_5) (**5-d_0**) to Cp*W(NO)($CHD_{syn}CMe_3$)(C_6D_5) (**5-d_6**) and Cp*W(NO)(CH_2CMe_3)(CH_2SiMe_3) (**4-d_0**) to Cp*W(NO)($CHD_{syn}CMe_3$)(CD_2SiMe_3-d_9) (**4-d_{12}**) product ratios are the average values obtained from multiple integrations of the fully resolved CH_{anti}H doublet and CH_{anti}D singlets. Two independent experiments were conducted for C_6H_6/C_6D_6, while the experiment in $SiMe_4$/$SiMe_4$-d_{12} was conducted only once. For **2** in C_6H_6/C_6D_6, the ratio of Cp*W(NO)($CH_2C_6H_5$)(C_6H_5) (**6-d_0**) to Cp*W(NO)($CHD_{syn}C_6H_5$)(C_6D_5) (**6-d_6**) was determined by integration of the combined overlapping H_{anti} signals for **6-d_0** and **6-d_6** vs the H_{syn} signal for **6-d_0**. The results from two independent experiments were averaged to give a ratio of 1.84(7):1, from which a H/D product ratio of 1.17(19) was calculated using a 0.99(5):1 integration for H_{syn} to H_{anti} obtained from a spectrum of pure **6-d_0** recorded under identical spectrometer conditions. The reported errors are standard errors in the mean and have been adjusted for sample size by multiplication of the appropriate Student t factor at the 95% confidence level.[40]

Preparation of Cp*W(NO)(CH_2CMe_3)(C_6D_5) (5-d_5). Complex **5-d_5** was prepared in a manner analogous to its protio analogue[38] via the reaction of Cp*W(NO)(CH_2CMe_3)Cl (0.135 g, 0.30 mmol) and $(C_6D_5)_2Mg\cdot x$(dioxane) (45 mg, 0.30 mmol) in Et_2O (10 mL). The crude residue was extracted with Et_2O (5 mL), and filtered through Celite (1 × 0.7 cm) rather than Florosil. The solvent was removed in vacuo to obtain an orange residue that was then recrystallized from hexanes to obtain red rosettes (68 mg, 46%).

^{1}H NMR (400 MHz, C_6D_6): δ − 2.05 (d, $^2J_{HH}$ = 11.4, 1H, CH_{syn}H), 1.26 (s, 9H, CMe_3), 1.53 (s, 15H, C_5Me_5), 4.50 (d, $^2J_{HH}$ = 11.4, 1H, CH_{anti}H). ^{2}H{^{1}H} NMR (61 MHz, C_6H_6): δ 7.10 (m, Ph D), 7.70 (br s, Ph D). Anal. Calcd for $C_{21}H_{26}D_5NOW$: C, 50.21; H/D,[39] 6.22; N, 2.79. Found: C, 50.24; H/D, 6.34; N, 2.87.

Preparation of Cp*W(NO)($CH_2C_6H_5$)(C_6D_5) (6-d_5). The reaction of Cp*W(NO)($CH_2C_6H_5$)Cl (0.145 g, 0.30 mmol) and $(C_6D_5)_2Mg\cdot x$(dioxane) (45 mg, 0.30 mmol) in THF (10 mL) for 6 h yielded a yellow-orange solid after workup. Repeated attempts to crystallize the resulting crude residue, including from neat Et_2O in the same manner as used for **6-d_6**,[6b] afforded only a small amount of semicrystalline orange solid (10 mg, 7%). The sample was determined to be ∼85% pure by ^{1}H NMR spectroscopy.

^{1}H NMR (400 MHz, C_6D_6): δ 1.53 (s, 15H, C_5Me_5), 2.12 (d, $^2J_{HH}$ = 6.4, 1H, CH_{syn}H), 3.41 (d, $^2J_{HH}$ = 6.4, 1H, CH_{anti}H), 6.50 (t, $^3J_{HH}$ = 7.8, 2H, Bzl H_{meta}), 6.84 (d, $^3J_{HH}$ = 7.6, 2H, Bzl H_{ortho}), 7.05 (t, $^3J_{HH}$ = 7.5, 2H, Bzl H_{para}). ^{2}H{^{1}H} NMR (61 MHz, C_6H_6): δ 6.9−7.2 (Ph D).

Thermolysis of 5-d_5 and 6-d_5. The thermolyses were conducted in a similar fashion as those for **1-d_4**. A J. Young NMR tube was charged with **5-d_5** or **6-d_5** (10−12 mg, 0.020−0.024 mmol), hexamethyldisilane (2 mg, 0.014 mmol), and either C_6D_6 or CD_2Cl_2 (0.8 mL). The thermolyses were conducted in the constant-temperature bath set to 70.0 °C, and the tubes were periodically removed to record ^{1}H NMR spectra at ambient temperatures. For **5-d_5**, the progress of the reaction was monitored for 5 h. New signals attributable to **5′-d_5** were observed to grow in simultaneously for H_{anti} at 4.37 ppm and Ph−H at 7.1 and 7.70 ppm. Average conversions of **5-d_5** to **5′-d_5** were determined from multiple integrations of the H_{anti} signals of **5-d_5** and **5′-d_5** at several time intervals. The relative standard deviations in the mean values were typically <5%. The observed rate constant for H/D exchange and the corresponding equilibrium constant were calculated from the experiment performed in CD_2Cl_2 via nonlinear-least-squares analysis of the plot of percent conversion vs time using Origin 5.0 software.[41] After 5 h, the solvent was removed in vacuo, and the residue was dissolved in C_6H_6 to record a ^{2}H{^{1}H} NMR spectrum which showed a new signal at −1.98 ppm corresponding to D_{syn} of **5′-d_5**. For **6-d_5**, the thermolysis was conducted under the same conditions for 45 h. A new signal attributable to CH_{anti}D of **6′-d_5** occurred was observed at 3.38 ppm. After 45 h, the solvent was replaced with C_6H_6 in order to record a ^{2}H{^{1}H} NMR spectrum. A resonance for CHD_{syn} of **6′-d_5** was evident at 2.17 ppm.

Theoretical Calculations Using the DFT Approach. All calculations were performed using Gaussian 98[42] on Intel PII PC computers employing the same method described by Poli and Smith.[8] All calculations utilized the LANL2DZ basis set and a DFT approach using the three-parameter exchange functional of Becke[43] and the correlation functional of Lee, Yang, and Parr (B3LYP).[44] The LANL2DZ basis set includes

(40) Harris, D. C. *Quantitative Chemical Analysis*, 2nd ed.; W. H. Freeman: New York, 1987; pp 44−55.
(41) Origin 5.0 Microcal Software Inc., 1991−1997.

both Dunning and Hay's D95 sets for H, C, N, and O[45] and the relativistic electron core potential (ECP) sets of Hay and Wadt for W.[46] The alkylidene fragment **C** has previously been optimized.[8] Frequency calculations on optimized species established that all the transition states possessed one and only one imaginary frequency and that the products and intermediates possessed no imaginary frequencies. The reported energies are calculated gas-phase free energies at standard temperature (298.15 K) and pressure (1 atm). Spatial plots of the optimized geometries and frontier orbitals were obtained from Gaussian 98 output using Molden v3.6.[47]

Acknowledgment. We are grateful to the Natural Sciences and Engineering Research Council of Canada for support of this work in the form of grants to P.L. and postgraduate scholarships to C.S.A. We thank Ms. E. Tran for her initial contributions to this work. We also thank Dr. K. M. Smith for his assistance with the DFT calculations and many helpful discussions.

Supporting Information Available: Tables giving kinetic data for the isomerization of **5-d_5** and pictures, Cartesian coordinates, and energies for all structures optimized by DFT calculations. This material is available free of charge via the Internet at http://pubs.acs.org.

OM010380C

(42) Frisch, M. J.; Trucks, G. W.; Schlegel, H. B.; Scuseria, G. E.; Robb, M. A.; Cheeseman, J. R.; Zakrzewski, V. G.; Montgomery, J. A., Jr.; Stratmann, R. E.; Burant, J. C.; Dapprich, S.; Millam, J. M.; Daniels, A. D.; Kudin, K. N.; Strain, M. C.; Farkas, O.; Tomasi, J.; Barone, V.; Cossi, M.; Cammi, R.; Mennucci, B.; Pomelli, C.; Adamo, C.; Clifford, S.; Ochterski, J.; Petersson, G. A.; Ayala, P. Y.; Cui, Q.; Morokuma, K.; Malick, D. K.; Rabuck, A. D.; Raghavachari, K.; Foresman, J. B.; Cioslowski, J.; Ortiz, J. V.; Stefanov, B. B.; Liu, G.; Liashenko, A.; Piskorz, P.; Komaromi, I.; Gomperts, R.; Martin, R. L.; Fox, D. J.; Keith, T.; Al-Laham, M. A.; Peng, C. Y.; Nanayakkara, A.; Gonzalez, C.; Challacombe, M.; Gill, P. M. W.; Johnson, B. G.; Chen, W.; Wong, M. W.; Andres, J. L.; Head-Gordon, M.; Replogle, E. S.; Pople, J. A. *Gaussian 98*, revision A.9; Gaussian, Inc.: Pittsburgh, PA, 1998.

(43) Becke, A. D. *J. Chem. Phys.* **1993**, *98*, 5648−5652.

(44) (a) Lee, C.; Yang, W.; Parr, R. G. *Phys. Rev.* **1988**, *B37*, 785−789. (b) Volko, S. H.; Wilk, L.; Nusair, N. *Can. J. Phys.* **1980**, *58*, 1200−1211.

(45) Dunning, T. H., Jr.; Hay, P. J. In *Modern Theoretical Chemistry*; Schaefer, H. F., III, Ed.; Plenum Press: New York, 1976; pp 1−28.

(46) (a) Hay, P, J.; Wadt, W. R. *J. Chem. Phys.* **1985**, *82*, 270−283. (b) Wadt, W. R.; Hay, P. J. *J. Chem. Phys.* **1985**, *82*, 284−298. (c) Hay, P. J.; Wadt, W. R. *J. Chem. Phys.* **1985**, *82*, 299−310.

(47) Schaftenaar, G.; Nordik, J. H. *J. Comput.-Aided Mol. Design* **2000**, *14*, 123−134.